

Instituto Tecnológico y de Estudios Superiores de Monterrey

Campus Monterrey

**School of Engineering and Sciences**



*The influence of pH in the kinetic characterization of thermophilic  
 $\beta$ -fructosidase from *T. maritima**

A thesis presented by

**Juan Jesús Cruz Maldonado**

Submitted to the

School of Engineering and Sciences

in partial fulfillment of the requirements for the degree of

**Master of Science in Biotechnology**

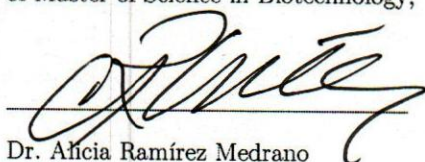
Monterrey Nuevo León, December 14<sup>th</sup>, 2018

# Instituto Tecnológico y de Estudios Superiores de Monterrey

Campus Monterrey

School of Engineering and Sciences

The committee members, hereby, certify that have read the thesis presented by Juan Jesús Cruz Maldonado and that it is fully adequate in scope and quality as a partial requirement for the degree of Master of Science in Biotechnology,

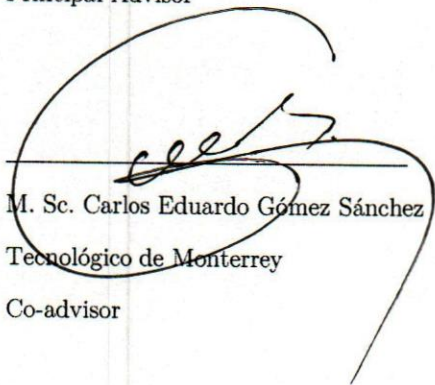


Dr. Alicia Ramírez Medrano

Tecnológico de Monterrey

School of Engineering and Sciences

Principal Advisor



M. Sc. Carlos Eduardo Gómez Sánchez

Tecnológico de Monterrey

Co-advisor



Dr. Oscar Alejandro Aguilar Jiménez

Tecnológico de Monterrey

Committee Member



Dr. Jorge Alejandro Benavides Lozano

Tecnológico de Monterrey

Committee Member



Dr. Rubén Morales Menéndez

Dean of Graduate Studies

School of Engineering and Sciences

Monterrey Nuevo León, December 14<sup>th</sup>, 2018



**Tecnológico  
de Monterrey**

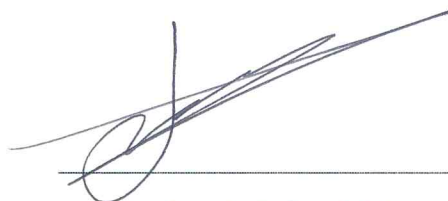
04 DIC 2018

**Dirección Nacional de Posgrado  
Dr. Rubén Morales Menéndez**

## Declaration of Authorship

I, Juan Jesús Cruz Maldonado declare that this thesis titled, "The influence of pH in the kinetic characterization of thermophilic  $\beta$ -fructosidase from *T. maritima*" and the work presented in it are my own. I confirm that:

- This work was done wholly or mainly while in candidature for a Master of Science degree at this University.
- Where any part of this thesis has previously been submitted for a degree or any other qualification at this University or any other institution, this has been clearly stated.
- Where I have consulted the published work of others, this is always clearly attributed.
- Where I have quoted from the work of others, the source is always given. With the exception of such quotations, this thesis is entirely my own work.
- I have acknowledged all main sources of help.
- Where the thesis is based on work done by myself jointly with others, I have made clear exactly what was done by others and what I have contributed myself.



Juan Jesús Cruz Maldonado

Monterrey Nuevo León, December 14<sup>th</sup>, 2018

©2018 by Juan Jesús Cruz Maldonado

All rights reserved

## Dedication

This thesis is dedicated to the most important people and main motivators in my life:

*Alma y Daniel, thank you for always being there for me, I'll always be by your side you too*

*Mom and dad, your unquantifiable and unconditional love gives me the motivation to excel  
every day.*

## Acknowledgements

I could never have finished this work without the support and guidance of so many people. First, I would like to recognize the ever-lasting backing of my family whose unconditional support encouraged me to always do better.

Of course, this could not have been possible without the scholarship granted by Tecnológico de Monterrey. Special mention to Campus Ciudad de México that aided me with some of the materials needed for the project and Campus Toluca that kindly let me work at their installations. Also, I want to express my gratitude to CONACyT for the financial support for living (CVU: 736486).

I would like to thank to my advisors: Dr. Alicia Ramírez whose support was important for the culmination of the project and M. Sc. Carlos Eduardo Gómez whose guidance and in-depth science talks were major motivational catalysts. I also want to acknowledge the effort and time dedicated by my dissertation committee, Dr. Alejandro Aguilar and Dr. Jorge Benavides, whose keen-eyed observations greatly improved this thesis.

I would also like to thank Lucero Jiménez, Paulina Ingelmo, Adiel Flores, Liliana Santos, Julio César Fabián and Alberto Yael Solís. Your support, orientation and partnership eased this path.

Last, but certainly not least, I want to thank Juan, María, Daniel and Alma for never letting me down and always cheer me up, even when things seemed gray. Thank you for everything and for every day.

*The influence of pH in the kinetic characterization of thermophilic  
β-fructosidase from T. maritima*

by

**Juan Jesús Cruz Maldonado**

**Abstract**

Given their advantageous features such as high reaction rates, increased specificity and negligible by-products generations, enzyme-catalyzed reactions are keep gaining ground over conventional chemical process. However, only a small fraction of currently known enzymes, is used in commercial processes at a large scale. Catalytic efficiency and stability reduction at drastic process conditions are some of the factors that restrain large scale biocatalysis boom. This can be exemplified in the industrial hydrolysis of sucrose where, at process conditions, *S. cerevisiae* β-fructosidase (BfrA) is subjected to thermal denaturation and substrate inhibition. In this regard, kinetic characterization of a thermophilic BfrA could help to overcome these inconveniences. Therefore, the main objective of this study is the kinetic characterization of *T. maritima* BfrA through a mathematical model that accounts for the simultaneous effects of pH and substrate inhibition over catalytic activity and kinetic parameters. Fitting of proposed model to experimental data yielded a surface of response which confirmed substrate uncompetitive inhibition at 146 mM of sucrose and optimum pH interval between 4.5 and 5.5. Estimation of kinetic parameters showed that  $K_m$  and  $K_i$  are slightly pH-dependent while  $v_{max}$  demonstrated to be sensitive to pH shifts. Likewise, estimated ionization constants of 3.0 and 6.60 suggested side-chain carboxylic groups of nucleophilic Asp and general acid/base Glu, which agreed with previous structural and mechanistic studies of *T. maritima* BfrA. These results suggest that the proposed model provide good estimations with respect of expected enzymatic activity of *T. maritima* BfrA at different conditions of pH and sucrose concentrations. Hence, can be useful for further kinetic characterization studies with potential application in biocatalysis process design.

Keywords: Kinetic characterization – pH-dependence – pKa – β-fructosidase – *Thermotoga maritima*

# *La influencia del pH en la caracterización cinética de la $\beta$ -fructosidasa termofílica de *T. maritima**

por

**Juan Jesús Cruz Maldonado**

## **Resumen**

Dadas sus características benéficas como altas velocidades de reacción, mayor especificidad y generación despreciable de subproductos, las reacciones catalizadas por enzimas siguen ganando terreno sobre los procesos químicos convencionales. Sin embargo, solo una pequeña fracción de las enzimas conocidas es usada en procesos comerciales a gran escala. La reducción en su eficiencia catalítica y estabilidad a condiciones drásticas de proceso son algunos de los factores que frenan el auge de la biocatálisis a gran escala. Esto se puede ver ejemplificado en la hidrólisis industrial de sacarosa en donde, a condiciones de proceso, la  $\beta$ -fructosidasa (BfrA) de *S. cerevisiae* está sometida a desnaturalización térmica e inhibición por sustrato. En este sentido, la caracterización cinética de una BfrA termofílica podría ayudar a superar estos inconvenientes. Por lo tanto, el objetivo principal de este trabajo es la caracterización cinética de una BfrA de *T. maritima* por medio de un modelo matemático que describa los efectos simultáneos del pH y la inhibición por sustrato sobre la actividad catalítica y los parámetros cinéticos. El ajuste del modelo propuesto a los datos experimentales produjo una superficie de respuesta confirmando la inhibición acompetitiva por sustrato a una concentración de 146 mM de sacarosa y el intervalo de pH óptimo entre 4.5 y 5.5. La estimación de los parámetros cinéticos mostró que  $K_m$  y  $K_i$  son ligeramente dependientes del pH, mientras que  $v_{max}$  fue sensible a los cambios de pH. Así mismo, las constantes de ionización estimadas de 3.0 y 6.60 sugirieron grupos carboxílicos de Asp nucleófilico y Glu como ácido/base general, coincidiendo con estudios estructurales y mecanísticos de BfrA de *T. maritima* previos. Estos resultados sugieren que el modelo propuesto proporciona buenas estimaciones con respecto a la actividad enzimática esperada de BfrA de *T. maritima* a diferentes condiciones de pH y concentraciones de sacarosa. Por lo tanto, puede ser útil para estudios subsecuentes de caracterización cinética con aplicación potencial en el diseño de procesos de biocatálisis.

## List of Figures

<i>Figure 1.1</i> Catalytic mechanism of an enzyme.....	12
<i>Figure 1.2</i> Schematic representation of enzyme stabilization approaches.....	15
Figure 1.3 Catalytic mechanism of sucrose hydrolysis in $\beta$ -fructosidase.....	17
<i>Figure 3.1</i> BfrA production and purification train.....	34
<i>Figure 4.1</i> Biomass (dry weight) and glucose profiles for bioreactor culture.....	38
<i>Figure 4.2</i> SDS-PAGE from soluble and purified fractions. Lane1: Soluble fraction. Lanes 2-4: Non-bound IMAC fractions. Lane 5: ECL Rainbow – High Range (GE®) molecular weight marker. Lane 6: (Dialyzed) IMAC eluted fraction. ....	40
<i>Figure 4.3</i> Example progress curve 146.11 mM sucrose and pH 5.56 .....	40
<i>Figure 4.4</i> Example plots of initial velocity against substrate (A) and pH (B) .....	41
<i>Figure 4.5</i> Plot of initial activity vs substrate concentration .....	43
<i>Figure 4.6</i> Surface of response (1 <sup>st</sup> model) and experimental data points (red dots) .....	44
<i>Figure 4.7</i> Surface of response (2 <sup>nd</sup> model) and experimental data points (red dots).....	46
<i>Figure 4.8</i> Apparent kinetic parameters against pH for the 1 <sup>st</sup> (triangles) and 2 <sup>nd</sup> (circles) model .....	49
<i>Figure D.1</i> IMAC chromatogram. 1-3: Non-bound eluted peaks. 4: Eluted peak. ....	62
<i>Figure E.1</i> Initial velocity against substrate plots (fixed pH). Experimental data and the resulting model from LSNLR are represented by the red dots and dashed blue line respectively .....	63
<i>Figure E.2 (Cont.)</i> Initial velocity against substrate plots (fixed pH). Experimental data and the resulting model from LSNLR are represented by the red dots and dashed blue line respectively.....	64
<i>Figure E.3</i> Initial velocity against pH plots (fixed substrate) .....	65
<i>Figure E.4 (Cont.)</i> Initial velocity against pH plots (fixed substrate).....	66

## List of Tables

<i>Table 3.1</i> Buffers solutions employed at each pH interval.....	36
<i>Table 4.1</i> BfrA Purification.....	39
<i>Table 4.2</i> Ionizable groups and their corresponding amino acid that could be present at the catalytic site. Modified from (Segel, 1975) .....	42
<i>Table 4.3</i> Estimated kinetic parameters (1 <sup>st</sup> model, 1 <sup>st</sup> approach) and sum of squared residuals ( $\chi^2$ ) .....	47
<i>Table 4.4</i> Estimated kinetic parameters (2 <sup>nd</sup> model, 1 <sup>st</sup> approach) and sum of squared residuals ( $\chi^2$ ).....	48
<i>Table 4.5</i> Estimated kinetic parameters (2 <sup>nd</sup> approach) and sum of squared residuals ( $\chi^2$ ).....	50
<i>Table 4.6</i> Estimated $pK_a$ values (2 <sup>nd</sup> model, 1 <sup>st</sup> approach).....	51
<i>Table 4.7</i> Estimated $pK_a$ values (2 <sup>nd</sup> approach).....	51
<i>Table 4.8</i> Amino acids in close contact with sucrose at the active site of BfrA (Alberto et al., 2004).....	52
<i>Table A.1</i> Abbreviations .....	57
<i>Table A.2</i> Acronyms .....	57
<i>Table A.3</i> Variables and symbols .....	58
<i>Table A.4</i> Polyacrylamide gel composition.....	59
<i>Table A.5</i> 1X running buffer composition .....	59
<i>Table A.6</i> 2X sample buffer composition.....	59
<i>Table A.7</i> Coomassie blue solution composition .....	60
<i>Table A.8</i> Destaining solutions composition.....	60
<i>Table A.9</i> Enzymatic assay buffers compositions. All quantities expressed for 1 L volume.....	60
<i>Table A.10</i> Biomass determination .....	61
<i>Table A.11</i> Glucose consumption .....	61

# Contents

Abstract.....	vi
Resumen .....	vii
List of Figures.....	viii
List of Tables.....	ix
Chapter 1. Introduction .....	12
1.1    Enzymes .....	12
1.2    Practical application of enzymes and its economic importance.....	13
1.3    Challenges for successful industrial biocatalysis.....	14
1.4    Industrial sucrose inversion.....	16
Chapter 2. Theoretical Framework.....	21
2.1    Kinetic characterization of the enzymes.....	21
Chapter 3. Materials and Methods .....	31
3.1    Reagents employed for enzymatic assays .....	31
3.2    Strains, plasmids and culture media .....	31
3.3 <i>E. coli</i> transformation protocol .....	32
3.4    Production of recombinant BfrA.....	33
3.5    BfrA purification.....	33
3.6    Analytic methods. ....	35
3.7    Enzymatic assays and experimental set-up.....	36
3.8    Model fitting and kinetic parameter estimation.....	37
Chapter 4. Results and Discussion.....	38

4.1	BfrA production and purification.....	38
4.2	Determination of BfrA catalytic activity .....	40
4.3	BfrA activity modelling.....	42
4.4	BfrA kinetic characterization .....	47
Chapter 5. Conclusions .....		54
A. Appendix A.....		57
	Abbreviations and acronyms.....	57
B. Appendix B.....		58
	Variables and Symbols.....	58
C. Appendix C.....		59
	Solutions and Buffers .....	59
D. Appendix D .....		61
	Production and Purification data.....	61
E. Appendix E.....		63
	Resulting plots of BfrA kinetic characterization .....	63
Bibliography .....		67
Submitted works.....		76
Curriculum Vitae.....		77

## Chapter 1. Introduction

### 1.1 Enzymes

Enzymes are proteins that serve as catalysts in living organisms' biochemical reactions involved in every metabolic pathway (Illanes, 2008). Hence, they are one of the most important homeostasis regulators, sustaining organism's life itself. As every other protein, enzymes' amino acid sequence defines their structural and biochemical properties. Despite their large molecular weights, catalytic regions within the enzyme are rather small and, in most of the cases, only one is present.

The active site, as it is known, comprises specific amino acids residues distributed in a very precise spatial arrangement enabling interaction with complementary groups of a certain substrate molecule (Lodish et al., 2008). Such features provide the enzyme increased specificity and high rate reactions, which can be  $10^5$  to  $10^8$  times faster than a normal chemical reaction (Gurung et al., 2013). An enzyme accelerates the rate of reaction, namely the amount of substrate molecules that are converted to product per unit of time, by decreasing the activation energy of the former (see *Figure 1.1*). Close interaction of active site amino acids and the substrate causes distortion of its bonds, making possible its transformation into product (Segel, 1975).

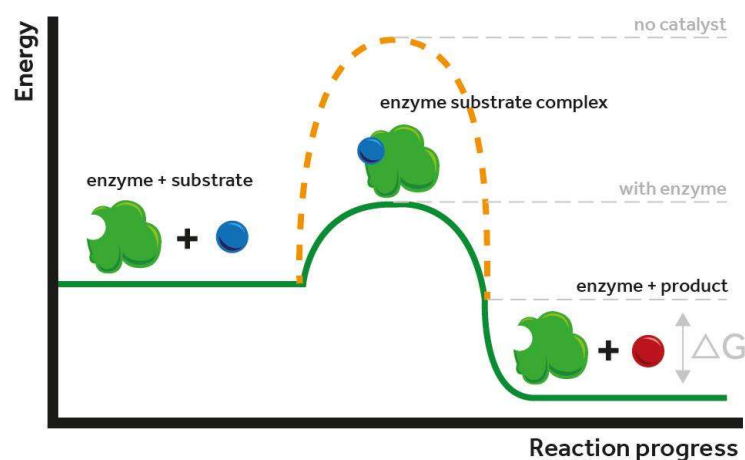


*Figure 1.1* Catalytic mechanism of an enzyme

These distinct characteristics determine the reaction that enzymes catalyze. In fact, general enzyme classification and their Enzyme Commission (EC) number are established according to the latter. Further classification specifies target molecules or groups that acts as either donors or acceptors of electrons. According to the International Union of Biochemistry and Molecular Biology (IUBMB) web page there are at least 6200 registered enzymes to this day (Moss, 2018).

## 1.2 Practical application of enzymes and its economic importance

Biocatalysis, namely the use of enzyme outside its natural environment, has been employed since ancient times for production of foods and beverages such as cheese, sourdough bread, wine and vinegar. However, it was not until the later part of the XIX century that structured investigations, aiming to elucidate enzyme's mechanism took place. Moreover, the first mathematical equation that described enzymatic reaction rate was developed at the beginning of the last century (Henri, 1902). The latter was reformulated by incorporating chemical equilibria (Michaelis & Menten, 1913) and steady state (Briggs & Haldane, 1925) concepts, resulting in both the Henri-Michaelis Menten and Brigg-Haldane equations both of which are still used today to describe enzyme's kinetic behavior.

With the development of new fermentation and purification methodologies, a wide amount of pure and characterized enzymes became more readily available for incorporation into industrial processes (Kirk et al., 2002). Some of the first examples of microbial enzymes produced in a commercial scale were protease and  $\alpha$ -amylase, used in the detergent and starch degradation industries respectively (Arbige & Pitcher, 1989). Likewise, development of recombinant DNA technology increased the spectrum of enzymes that could be isolated and characterized. Given its advantageous features such as quick and straightforward genome modification, rapid growth to high cell densities, ease of culture in inexpensive media and high recombinant protein accumulation (Rosano & Ceccarelli, 2014), *E. coli* has remained as the predilect organism for recombinant protein expression, enzymes included.

Since enzymes display high reaction rates and substrate specificity in aqueous environments at moderate conditions (i.e. pH, temperature, pressure), conventional chemical reactions in organic media at extreme process conditions became less common (Sanchez & Demain, 2016). Moreover, enzyme's biological nature and lack of reaction by-products make them suitable for environmentally friendly industrial process development (Wohlgemuth, 2010). Altogether, these features derived in a myriad of industrial processes harnessing enzymes in applications ranging from simpler juice clarification and flavor enhancement to more complex biofuels production and pharmaceuticals synthesis (Choi et al., 2009).

Nowadays, enzymatic industrial processes keep gaining importance, as evidenced by rapid growth of the global market for industrial enzymes which was valued in \$4.2 billion for the year 2014 and it is expected to grow to 6.3 billion dollars by the year 2022 (Markets and Markets, 2017; Singh et al., 2016). Despite this generalized growth, major enzyme-related industries are located in the US, Europe and Japan with some recent contribution of Asian companies (BBC-Business Communications Company Inc., 2009; Sarrouh, 2012).

According to information of Instituto Nacional de Estadística y Geografía (INEGI) Mexico's demand for enzymes in the year 2014 accounted for almost 2 billion pesos worth in imports. In contrast, only half a billion pesos worth in enzyme's exports was registered in the same year. Particularly, for hydrolytic enzymes such as chymotrypsin and invertase, about 8 kg were imported whereas only 1 kg of nationally produced enzymes were exported (INEGI, 2014b, 2014a). This data suggests both Mexico's high demand for industrial enzymes and a lack of suitable industrial enzymatic processes.

### 1.3 Challenges for successful industrial biocatalysis

Even though an estimate of 3000 enzymes have been characterized to date, only 5% of them are used commercially (Binod et al., 2013). Since enzymes have naturally evolved to work optimally

under physiological conditions, thight regulation of their catalytic efficiency and stability is exerted by temperature, pH and reactants concentration (Illanes, 2008). However, in order to be considered as profitable, industrial biocatalysis processes require an enzyme to work outside its physiological limits, which usually decreases both its efficiency and stability (Jemli et al., 2016). Such catalytic reduction will traduce in eventual enzyme replacement, which in the long term might become a big share of the production cost, especially for expensive enzymes. Thus, from the perspective of large-scale industrial processes, cost-effective biocatalysis is achieved only by enzymes capable to maintain both catalytic efficiency and stability at rather drastic process conditions (Woodley, 2013). Although chemical modification and medium engineering have been used to increase enzyme's stability (see *Figure 1.2*), immobilization and protein engineering remain as the most employed approaches (Choi et al., 2015; Silva et al., 2018).

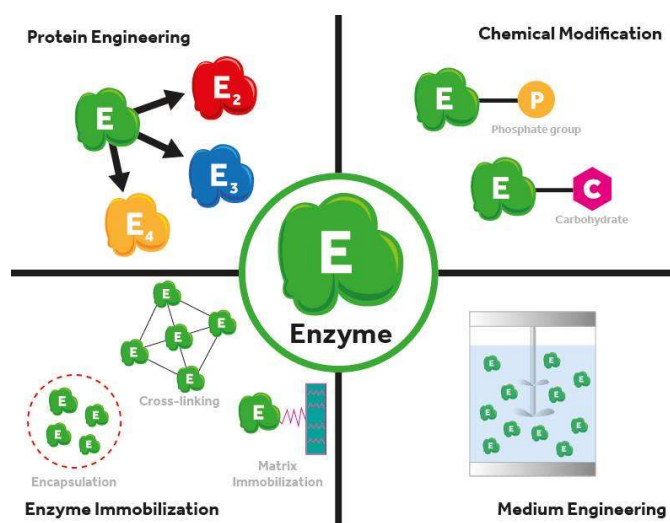


**Figure 1.2** Schematic representation of enzyme stabilization approaches

Immobilization facilitates both process engineering for either batch or continuous operation and the use and recovery of the enzyme (Di Cosimo et al., 2013). Since immobilization is feasible only when the enzyme's catalytic properties are maintained (Mateo et al., 2007), various immobilization methodologies have aimed to modify not only enzyme's stability but also its activity, specificity or a combination of these (Garcia-Galan et al., 2011; Rodrigues et al., 2013).

Although the latter approach is usually straightforward and can attain high reproducibility, it is still limited by activity loss during immobilization and, perhaps more importantly, enzyme's native kinetic characteristics. In this regard, protein engineering attempts to change enzyme's traits by introducing modifications, via recombinant DNA technology, in its primary structure (Bommarius & Paye, 2013). This methodology is subdivided into three main categories: rational design, semi-rational design and directed evolution. Each of them having a trade-off between enzyme's structural and functional knowledge and robust high throughput technologies (Liu, Xun, & Feng, 2018).

Another approach that has started to trend recently is the use of enzymes from organisms capable to thrive at extreme environmental conditions, namely extremophiles. Employing this type of enzymes is advantageous given that they already display stability at extreme conditions of salinity, pH and/or temperature (Demirjian et al., 2001; Van den Burg, 2003). Hence, reducing the need of stability enhancement through protein engineering approaches. However, culture and maintenance of extremophiles pose a difficult task that requires of special equipment and growth media which usually yields insufficient enzyme for characterization and purification studies. Therefore, isolation and overexpression of coding genes for the target enzymes in model organisms such as *E. coli* is preferred (Adams et al., 1995). Altogether, these attractive characteristics have resulted in a growing interest for the incorporation of enzymes from extremophile organisms into industrial processes (Elleuche et al., 2014; Siddiqui, 2015).

#### 1.4 Industrial sucrose inversion

Sucrose or table sugar is a widely commercialized disaccharide naturally occurring in sugarcane and sugar beets. Sucrose hydrolysis produces an equimolar mixture of glucose and fructose which is commonly known as invert sugar due to optical activity change from sucrose's dextrorotatory to slightly levorotatory (Clarke, 1995). Invert sugar solution is quite hygroscopic, much sweeter than

sucrose and capable of increasing sugars' solubility. These features have been widely harnessed by food industry for the production of jams, soft-core candies, chocolates and cookies (Edwards, 2009; Nadeem et al., 2015).

Even though acid catalysis was initially used for sucrose inversion at an industrial scale, the need of highly concentrated acid solutions resulted in undesirable color and flavor alterations. In this regard, enzyme-catalyzed hydrolysis by  $\beta$ -fructosidase (BfrA) or invertase from *S. cerevisiae*, emerged as a more suitable alternative that eliminated acid catalysis inconveniences (Combes & Monsan, 1983; Dickensheets et al., 1977). Additionally, since reaction could be stopped simply by heating the solution and removal of the enzyme is not needed, enzymatic sucrose inversion posed advantageous unit operation simplification (Paine et al., 1925).

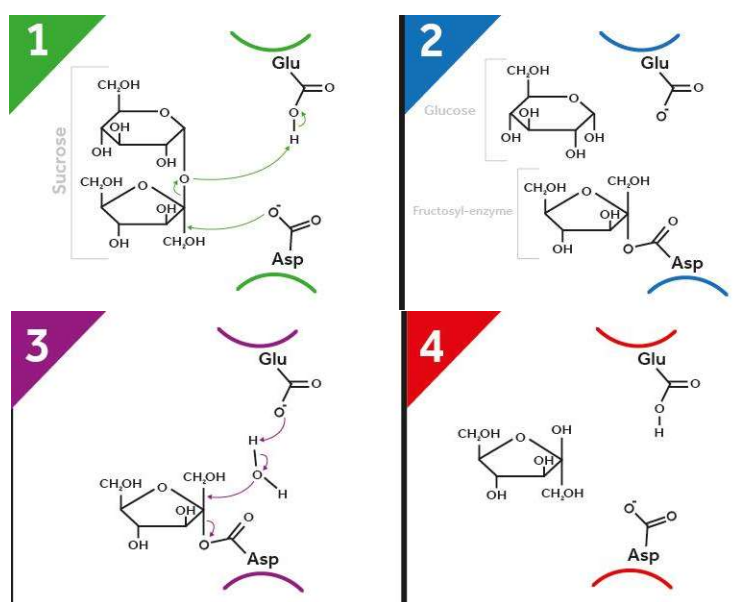


**Figure 1.3** Catalytic mechanism of sucrose hydrolysis in  $\beta$ -fructosidase

Invertase belongs to a group of more than 370 glycoside hydrolases named GH32 family, that break down carbohydrates. Despite its large number, enzymes of this family are related to their characteristic catalytic acidic residues. In the case of BfrA, these have been found to belong to Glu

and Asp which work as general acid/base and nucleophile respectively (Alberto et al., 2004; Reddy & Maley, 1990, 1996). Although two catalytic mechanisms, namely inverting and retaining, are found among glycoside hydrolases (Davies & Henrissat, 1995; Zechel & Withers, 2000), enzymes of the GH32 family operate solely through a retaining mechanism (Koshland & Stein, 1954). Particularly, sucrose hydrolysis via BfrA follows a double displacement mechanism. In a first step, protonation of the glycosidic oxygen of sucrose and nucleophilic attack of the C-2 fructose moiety is undergone by side-chain carboxylic groups of Glu and Asp respectively. As a result, glucose is released while a covalent fructosyl-enzyme complex is formed. In the second step, water molecule deprotonation by Glu enables hydrolysis of the glycosidic bond between fructose and Asp leading to fructose release and enzyme regeneration.

On the other hand, cost-effective enzymatic sucrose inversion process at an industrial scale demands processing of highly concentrated sucrose solutions usually between 60-70 % (w/v), preventing further dilution or concentration steps (Monsan & Combes, 1984). Also, processing at temperatures between 60-65 °C is desirable since it lowers contamination probability and solution's viscosity which in turn increases sucrose's mass transfer and, more importantly, the reaction rate (Gomes & Steiner, 2004; Rampp et al., 2000).

Since these process conditions are strange for the enzyme, some degree of activity reduction is expected. For instance, at high sucrose concentrations (i.e. 5-10 % (w/v)) BfrA exhibits uncompetitive substrate inhibition (Bowski et al., 1971; Combes & Monsan, 1983; Dickensheets et al., 1977; Liebl et al., 1998; Menéndez et al., 2013; Nadeem et al., 2015). Likewise, high temperature processing above 50-55 °C derives in irreversible inactivation of *S. cerevisiae* BfrA (Cavaille & Combes, 1995) which is evidenced by the drastic change in enzyme's half-lives from 10-11 h at 50°C to only 16-60 min at 60 °C (Akgöl et al., 2001; Amaya-Delgado et al., 2006). This time-dependent catalytic efficiency decay derives in constant replacement of inactivated enzyme increasing both production and processing costs.

To overcome BfrA thermal instability chemical modifications (Tananchai & Chisti, 2010), protein engineering (Mohandesi et al., 2017) and mostly immobilization approaches (Ahmad et al., 2001; Bayramoglu et al., 2017; Mafra et al., 2018; Valerio et al., 2013) have been explored. Regardless, few reports have investigated utilization of BfrA from extremophile organisms (Liebl et al., 1998; Menéndez et al., 2013). For instance the thermophilic bacteria *Thermotoga maritima*, originally isolated from volcanic ocean floor, has the highest number of carbohydrate degrading enzymes in a prokaryotic genome (Nelson et al., 1999). This feature makes it a very attractive organism for the search and characterization of thermophilic enzymes (Ballschmiter et al., 2006; Chen et al., 2015; Khan et al., 2007; Rajashekhara et al., 2002; Sun et al., 2012). Particularly, its BfrA displays good catalytic activity and stability at high temperatures evidenced by half-live times ranging from 32 h at 60 °C to 3 h at 90 °C (Liebl et al., 1998).

On the other hand, as mentioned above, ionization state of catalytically active residues is of utmost importance for BfrA activity. Hence, regarding kinetic characterization studies, medium pH is another important parameter to bear in mind. Even though the effect of pH has been addressed in earlier studies of *T. maritima* BfrA (Liebl et al., 1998; Menéndez et al., 2013), these have focused solely in determining an optimum pH for catalytic activity at arbitrary fixed conditions. Therefore, leaving out exploration of the pH-dependence of ionization constants and other equally important kinetic constants such as  $v_{max}$  and  $K_m$  (Knowles, 1976).

Due to its desirable features, utilization of *T. maritima* BfrA as a potential biocatalyst for industrial sucrose inversion is proposed. Hence, kinetic characterization of a recombinant version of *T. maritima* BfrA became the main objective of this study. For this purpose, production and partial purification of the enzyme took place. In parallel, a suitable velocity equation accounting for the simultaneous effects of pH and sucrose concentration was established. Moreover, measurement of BfrA initial rate of reaction at different substrate concentrations and pH conditions was performed

---

in a randomized order. Then, velocity equation was fitted to experimental data through non-linear regression via a computational software and parameters were estimated. Finally, it is suggested that determination of ionization constants (as explained in the following chapter) will yield important data about the functional groups and their respective amino acids involved in enzyme catalysis as well as substrate binding and inhibition. Such information coupled with knowledge of catalytic aminoacid roles in the reaction would be a useful tool for designing a biocatalysis process in regard of pH conditions.

Following sections provide detailed information regarding the study conducted. The theoretical framework addresses enzyme kinetics theory employed as well as establishment of *T. maritima* BfrA sucrose inversion reaction and subsequent deduction of the velocity equation. Materials and methods describe the procedures performed and the computational tools employed. Relevant findings in regard of kinetic characterization of the enzyme are showed in results and discussion section. Finally, concluding remarks as well as future perspectives concerning to this work can be found in the conclusions section. Additionally, data generated in this project along with detailed composition of solutions employed can be found in the appendix section.

## Chapter 2. Theoretical Framework

### 2.1 Kinetic characterization of the enzymes

Understanding enzyme's reaction rate mechanism is mandatory prior biocatalysis application for either laboratory studies or industrial scale processes (Illanes, 2008). As any other model aiming to describe a physicochemical phenomenon, velocity equations should be constructed around measurable parameters involved in the catalysis and delimited by educated assumptions regarding assay conditions.

General outlines on the analysis of enzyme kinetics found in literature provide some discrete examples of rate equations (Leskovac, 2003; Segel, 1975). However, since no enzyme nor reaction environment is the same, analysis of each system is required to yield appropriate velocity equations. For instance, consider the unireactant conversion of substrate into product by an enzyme that requires no cofactors nor activators:



Where  $S$ ,  $E$  and  $ES$  refer to the substrate, enzyme and enzyme-substrate complex respectively. Rates of formation and dissociation of the  $ES$  complex are described by  $k_1$  and  $k_{-1}$  respectively whilst  $k_P$  is the catalytic reaction rate. Before proceeding any further some considerations should be established:

- Enzyme, substrate and enzyme-substrate complex are under rapid equilibrium.
- Breakdown of the enzyme-substrate complex to enzyme and product is the limiting step of the reaction ( $k_P \ll k_{-1}$ ).
- Substrate concentration is much larger than enzyme's ( $[S] \gg [E]$ ), hence, formation of  $[ES]$  practically doesn't affect substrate concentration at early stages of reaction ( $[S_0] \approx [S]$ ).

- Since initial reaction rates are measured, conversion of  $P$  to  $S$  is negligible. In other words, there is no reverse reaction.

Applying the above-mentioned considerations, the reaction can be rewritten to:

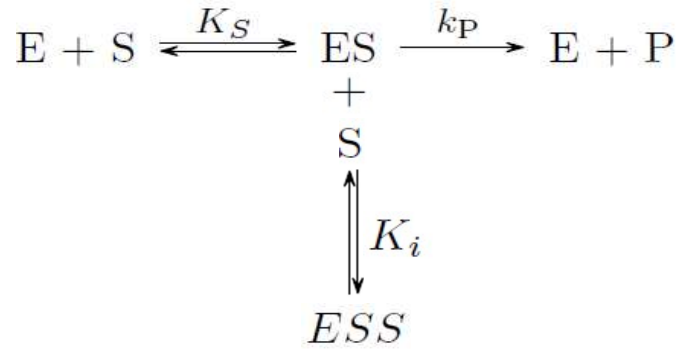


Hence, velocity equation for an unireactant enzyme is:

$$v = \frac{v_{max}[S]}{K_S + [S]} \quad (1)$$

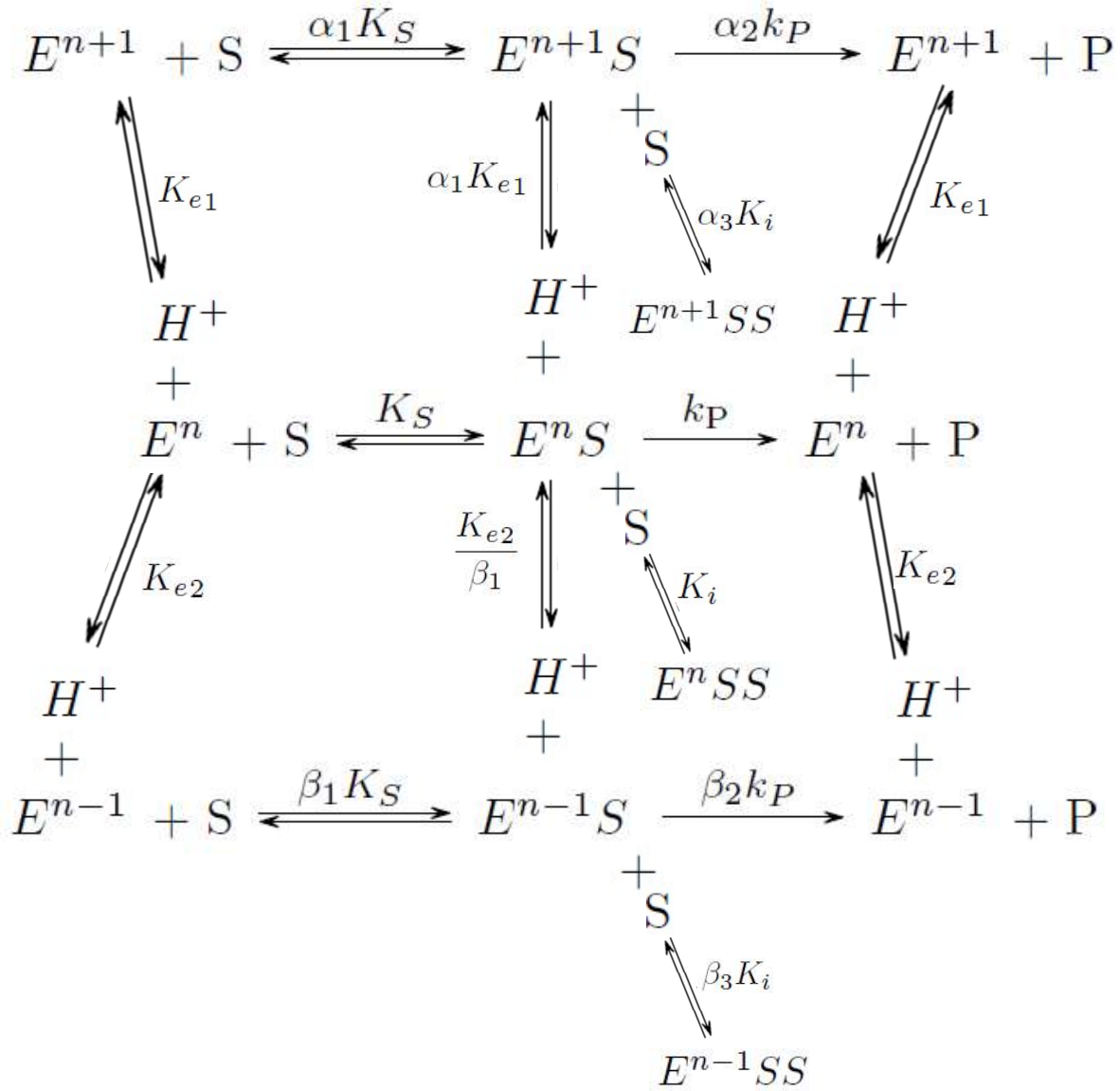
Where  $[S]$  is the substrate molar concentration,  $K_S$  the substrate affinity constant and  $v$  and  $v_{max}$  are the initial and maximum molar reaction rates respectively. It should be noted that, in practice,  $k_P$  and  $k_{-1}$  are frequently the same order of magnitude. Thus, instead of rapid equilibrium considerations, a steady-state treatment should be performed to obtain reaction rate equations. However, in most situations, resulting velocity equations from each of these methodologies are practically the same. Moreover, rapid equilibrium treatment is the most straightforward method to derive velocity equations from simple equilibria analysis between enzyme species (Segel, 1975). The latter comes in handy when magnitudes of rate constants are not known and is also applicable to complex multiligand systems. Therefore, rapid equilibrium treatment will continue to be employed for determination of velocity equations for the rest of this section.

Note that (1) practically is the Michaelis-Menten equation (Michaelis & Menten, 1913) which is capable of describe reaction rates only under very special conditions that are usually not met in industrial processes. For instance, BfrA reaction rate is affected by uncompetitive substrate inhibition at high sucrose concentrations (Bowski et al., 1971; Combes & Monsan, 1983; Paine et al., 1925). Therefore, reaction should be rewritten to consider this effect which in turn changes the form of the velocity equation to that of (2).



$$v = \frac{v_{max}[S]}{K_S + [S] + \frac{[S]^2}{K_i}} \quad (2)$$

The term  $K_i$  is the substrate inhibition constant that describes the equilibrium between  $ES$ ,  $S$  and  $ESS$  which is considered catalytically inactive. Equations (1) and (2), however, consider parameters such as temperature and pH to remain fixed. Since amino acids' ionizable groups provide the active site with a suitable structure for substrate binding and catalysis, changes in the surrounding pH would alter their ionic form leading to modification of enzyme's catalytic activity, stability or even substrate affinity (Cleland, 1977; Søndergaard et al., 2008). Therefore, examination on the effect of pH over enzyme's activity and estimated kinetic parameters such as  $v_{max}$ ,  $K_S$  and  $K_i$  are relevant for a kinetic characterization study with aim for industrial applications. Hence, for the analysis of BfrA velocity equation, pH effect is considered in the reaction by including protonated and deprotonated species of the enzyme ( $E^{n+1}$ ,  $E^{n-1}$ ) and the enzyme-substrate complex ( $ES^{n+1}$ ,  $ES^{n-1}$ ):



Before starting the deduction of the velocity equation, additional assumptions should be considered:

- $S$  has essentially the same charge, at least in the pH interval analyzed
- Reactions involving the addition or dissociation of  $H^+$  are much faster in comparison to the catalytic steps. Hence, they are in equilibrium and denoted by constants  $K_{e1}$  and  $K_{e2}$ .

Once assumptions are settled, deduction of BfrA velocity equation can be addressed. First, molar mass balance for the total amount of enzyme  $[E]_t$  and velocity dependence equations are established:

$$[E]_t = [E^n] + [E^{n+1}] + [E^{n-1}] + [E^n S] + [E^{n+1} S] + [E^{n-1} S] \quad (3)$$

$$v = k_P[E^n S] + \alpha_2 k_P[E^{n+1} S] + \beta_2 k_P[E^{n-1} S] \quad (4)$$

Then, equilibria relationships for each enzyme species are settled:

$$[E^n S] = \frac{[E^n][S]}{K_S} \quad (5)$$

$$[E^{n+1}] = \frac{[H^+][E^n]}{K_{e1}} \quad (6)$$

$$[E^{n-1}] = \frac{[E^n]K_{e2}}{[H^+]} \quad (7)$$

$$[E^{n+1} S] = \frac{[E^{n+1}][S]}{\alpha_1 K_S} \quad (8)$$

$$[E^{n-1} S] = \frac{[E^{n-1}][S]}{\beta_1 K_S} \quad (9)$$

$$[E^n SS] = \frac{[E^n S][S]}{K_i} \quad (10)$$

$$[E^{n+1} SS] = \frac{[E^{n+1} S][S]}{\alpha_3 K_i} \quad (11)$$

$$[E^{n-1} SS] = \frac{[E^{n-1} S][S]}{\beta_3 K_i} \quad (12)$$

By substituting (5), (6) and (7) in equations (8) to (12), each definition would be in terms of the free enzyme  $[E^n]$  and Hydrogen ion  $[H^+]$  molar concentrations:

$$[E^{n+1}S] = \frac{[E^n][H^+][S]}{\alpha_1 K_S K_{e1}} \quad (13)$$

$$[E^{n-1}S] = \frac{[E^n][S]K_{e2}}{\beta_1 K_S [H^+]} \quad (14)$$

$$[E^n SS] = \frac{[E^n][S]^2}{K_S K_i} \quad (15)$$

$$[E^{n+1}SS] = \frac{[E^n][H^+][S]^2}{\alpha_3 \alpha_1 K_S K_i K_{e1}} \quad (16)$$

$$[E^{n-1}SS] = \frac{K_{e2}[E^n][S]^2}{\beta_1 \beta_3 K_S K_i [H^+]} \quad (17)$$

By dividing (4) in (3) and substituting each enzyme species definition:

$$\frac{v}{[E]_t} = \frac{k_P[E^n S] + \alpha_2 k_P[E^{n+1}S] + \beta_2 k_P[E^{n-1}S]}{[E^n] + [E^{n+1}] + [E^{n-1}] + [E^n S] + [E^{n+1}S] + [E^{n-1}S] + [E^n SS] + [E^{n+1}SS] + [E^{n-1}SS]} \quad (18)$$

$$\frac{v}{[E]_t} = \frac{k_P \frac{[E^n][S]}{K_S} + \alpha_2 k_P \frac{[E^n][H^+][S]}{\alpha_1 K_S K_{e1}} + \beta_2 k_P \frac{[E^n][S]K_{e2}}{\beta_1 K_S [H^+]}}{[E^n] + \frac{[E^n][H^+]}{K_{e1}} + \frac{[E^n]K_{e2}}{[H^+]}} + \frac{[E^n][S]}{K_S} + \frac{[E^n][H^+][S]}{\alpha_1 K_S K_{e1}} + \frac{[E^n][S]K_{e2}}{\beta_1 K_S [H^+]} + \frac{[E^n][S]^2}{K_S K_i} + \frac{[E^n][H^+][S]^2}{\alpha_3 \alpha_1 K_S K_i K_{e1}} + \frac{K_{e2}[E^n][S]^2}{\beta_1 \beta_3 K_S K_i [H^+]}} \quad (18.1)$$

The  $[E^n]$  term can be eliminated by factorizing from numerator and denominator of the right-hand side of equation (18.1):

$$\frac{v}{[E]_t} = \frac{k_P \frac{[S]}{K_S} + \alpha_2 k_P \frac{[H^+][S]}{\alpha_1 K_S K_{e1}} + \beta_2 k_P \frac{[S]K_{e2}}{\beta_1 K_S [H^+]}}{1 + \frac{[H^+]}{K_{e1}} + \frac{K_{e2}}{[H^+]}} + \frac{[S]}{K_S} + \frac{[H^+][S]}{\alpha_1 K_S K_{e1}} + \frac{[S]K_{e2}}{\beta_1 K_S [H^+]} + \frac{[S]^2}{K_S K_i} + \frac{[H^+][S]^2}{\alpha_3 \alpha_1 K_S K_i K_{e1}} + \frac{K_{e2}[S]^2}{\beta_1 \beta_3 K_S K_i [H^+]}} \quad (18.2)$$

From the right-hand side of equation (18.2), the term  $k_P[S]$  can be factorized from the numerator while  $K_S$  is multiplied in both the numerator and the denominator:

$$\frac{v}{[E]_t} = \frac{k_P[S] \left( \frac{1}{K_S} + \frac{\alpha_2[H^+]}{\alpha_1 K_S K_{e1}} + \frac{\beta_2 K_{e2}}{\beta_1 K_S [H^+]} \right)}{1 + \frac{[H^+]}{K_{e1}} + \frac{K_{e2}}{[H^+]} + \frac{[S]}{K_S} + \frac{[H^+][S]}{\alpha_1 K_S K_{e1}} + \frac{[S]K_{e2}}{\beta_1 K_S [H^+]} + \frac{[S]^2}{K_S K_i} + \frac{[H^+][S]^2}{\alpha_3 \alpha_1 K_S K_i K_{e1}} + \frac{K_{e2}[S]^2}{\beta_1 \beta_3 K_S K_i [H^+]}} \quad (18.3)$$

$$\frac{v}{[E]_t} = \frac{k_P[S] \left( 1 + \frac{\alpha_2[H^+]}{\alpha_1 K_{e1}} + \frac{\beta_2 K_{e2}}{\beta_1 [H^+]} \right)}{K_S + \frac{K_S[H^+]}{K_{e1}} + \frac{K_S K_{e2}}{[H^+]} + [S] + \frac{[H^+][S]}{\alpha_1 K_{e1}} + \frac{[S]K_{e2}}{\beta_1 [H^+]} + \frac{[S]^2}{K_i} + \frac{[H^+][S]^2}{\alpha_3 \alpha_1 K_i K_{e1}} + \frac{K_{e2}[S]^2}{\beta_1 \beta_3 K_i [H^+]}} \quad (18.4)$$

Separation of terms can be done in the denominator of the right-hand side of equation (18.4) by factorizing  $K_S$ ,  $[S]$  and  $[S]^2/K_i$ :

$$\frac{v}{[E]_t} = \frac{k_P[S] \left( 1 + \frac{\alpha_2[H^+]}{\alpha_1 K_{e1}} + \frac{\beta_2 K_{e2}}{\beta_1 [H^+]} \right)}{K_S \left( 1 + \frac{[H^+]}{K_{e1}} + \frac{K_{e2}}{[H^+]} \right) + [S] \left( 1 + \frac{[H^+]}{\alpha_1 K_{e1}} + \frac{K_{e2}}{\beta_1 [H^+]} \right) + \frac{[S]^2}{K_i} \left( 1 + \frac{[H^+]}{\alpha_1 \alpha_3 K_{e1}} + \frac{K_{e2}}{\beta_1 \beta_3 [H^+]} \right)} \quad (18.5)$$

If each factor at the denominator and the numerator are defined as  $a$ ,  $b$ ,  $c$  and  $d$ . And by substituting in (18.5):

$$a = 1 + \frac{[H^+]}{K_{e1}} + \frac{K_{e2}}{[H^+]} \quad (19)$$

$$b = 1 + \frac{[H^+]}{\alpha_1 K_{e1}} + \frac{K_{e2}}{\beta_1 [H^+]} \quad (20)$$

$$c = 1 + \frac{[H^+]}{\alpha_1 \alpha_3 K_{e1}} + \frac{K_{e2}}{\beta_1 \beta_3 [H^+]} \quad (21)$$

$$d = 1 + \frac{\alpha_2[H^+]}{\alpha_1 K_{e1}} + \frac{\beta_2 K_{e2}}{\beta_1 [H^+]} \quad (22)$$

$$\frac{v}{[E]_t} = \frac{k_P [S] (d)}{K_S (a) + [S] (b) + \frac{[S]^2}{K_i} (c)} \quad (18.6)$$

By dividing the numerator and the denominator of the right-hand side of equation (18.6) by  $d$  and multiplying  $[E]_t$  to both sides of the equation:

$$v = \frac{v_{max} [S]}{K_S \left( \frac{a}{d} \right) + [S] \left( \frac{b}{d} \right) + \frac{[S]^2}{K_i} \left( \frac{c}{d} \right)} \quad (18.7)$$

Dividing the factor that multiplies  $[S]$  in both the denominator and the numerator results in:

$$v = \frac{v_{max} [S] \left( \frac{d}{b} \right)}{K_S \left( \frac{a}{b} \right) + [S] + \frac{[S]^2}{K_i} \left( \frac{c}{b} \right)} \quad (18.8)$$

Substituting the definitions for  $a$ ,  $b$ ,  $c$  and  $d$  in (18.8):

$$v = \frac{v_{max} [S] \left( \frac{1 + \frac{\alpha_2 [H^+]}{\alpha_1 K_{e1}} + \frac{\beta_2 K_{e2}}{\beta_1 [H^+]}}{1 + \frac{[H^+]}{\alpha_1 K_{e1}} + \frac{K_{e2}}{\beta_1 [H^+]}} \right)}{K_S \left( \frac{1 + \frac{[H^+]}{K_{e1}} + \frac{K_{e2}}{[H^+]}}{1 + \frac{[H^+]}{\alpha_1 K_{e1}} + \frac{K_{e2}}{\beta_1 [H^+]}} \right) + [S] + \frac{[S]^2}{K_i} \left( \frac{1 + \frac{[H^+]}{\alpha_1 \alpha_3 K_{e1}} + \frac{K_{e2}}{\beta_1 \beta_3 [H^+]}}{1 + \frac{[H^+]}{\alpha_1 K_{e1}} + \frac{K_{e2}}{\beta_1 [H^+]}} \right)} \quad (18.9)$$

Now by defining the following equilibrium constants for substrate binding, catalysis and inhibition and substituting them in (18.9), equation (18.10) is obtained:

$$K_{es1} = \alpha_1 K_{e1} \quad (23)$$

$$K_{es2} = \frac{K_{e2}}{\beta_1} \quad (24)$$

$$K_{v1} = \frac{\alpha_1 K_{e1}}{\alpha_2} \quad (25)$$

$$K_{v2} = \frac{\beta_2 K_{e2}}{\beta_1} \quad (26)$$

$$K_{ess1} = \alpha_1 \alpha_3 K_{e1} \quad (27)$$

$$K_{ess2} = \frac{K_{e2}}{\beta_1 \beta_3} \quad (28)$$

$$v = \frac{v_{max}[S] \left( \frac{1 + \frac{[H^+]}{K_{v1}} + \frac{K_{v2}}{[H^+]}}{1 + \frac{[H^+]}{K_{es1}} + \frac{K_{es2}}{[H^+]}} \right)}{K_S \left( \frac{1 + \frac{[H^+]}{K_{e1}} + \frac{K_{e2}}{[H^+]}}{1 + \frac{[H^+]}{K_{es1}} + \frac{K_{es2}}{[H^+]}} \right) + [S] + \frac{[S]^2}{K_i} \left( \frac{1 + \frac{[H^+]}{K_{ess1}} + \frac{K_{ess2}}{[H^+]}}{1 + \frac{[H^+]}{K_{es1}} + \frac{K_{es2}}{[H^+]}} \right)} \quad (18.10)$$

The latter equation can be expressed in terms of apparent kinetic parameters:

$$v = \frac{v_{max}^{app}[S]}{K_S^{app} + [S] + \frac{[S]^2}{K_i^{app}}} \quad (18.11)$$

Which are defined as follows:

$$v_{max}^{app} = v_{max} \left( \frac{1 + \frac{[H^+]}{K_{v1}} + \frac{K_{v2}}{[H^+]}}{1 + \frac{[H^+]}{K_{es1}} + \frac{K_{es2}}{[H^+]}} \right) \quad (29)$$

$$K_S^{app} = K_S \left( \frac{1 + \frac{[H^+]}{K_{e1}} + \frac{K_{e2}}{[H^+]}}{1 + \frac{[H^+]}{K_{es1}} + \frac{K_{es2}}{[H^+]}} \right) \quad (30)$$

$$K_i^{app} = K_i \left( \frac{1 + \frac{[H^+]}{K_{es1}} + \frac{K_{es2}}{[H^+]}}{1 + \frac{[H^+]}{K_{ess1}} + \frac{K_{ess2}}{[H^+]}} \right) \quad (31)$$

Close inspection of equation (18.10) shows its dependency on both substrate and hydrogen ion concentration, the latter, is directly related to the pH as expressed by equation (32). Hence, velocity equation obtained could describe BfrA reaction rate in the presence of effects of substrate inhibition and pH changes.

$$pH = -\log([H^+]) \quad (32)$$

Even though some kinetic characterization studies report the effect of pH over BfrA activity, their approach focuses almost exclusively in measurements of residual velocity at fixed substrate concentrations (Liebl et al., 1998; Martínez et al., 2014; Menéndez et al., 2013). This approach overlooks the effect of pH over kinetic parameters such as  $v_{max}$ ,  $K_S$  and  $K_i$  and estimation of ionization constants (i.e.  $K_{e1}$ ,  $K_{e2}$ ). The latter could provide information about the  $pK_a$  values of the ionizable groups and, therefore, the amino acids involved in catalysis, substrate binding and, in this case, substrate inhibition (Cleland, 1982; Leskovac, 2003; Segel, 1975). Such data would serve as a guideline for enzymatic activity modelling and process design. To date, no previous study has dealt with the kinetic characterization of *T. maritima* BfrA under simultaneous substrate inhibition and shifting pH conditions.

## Chapter 3. Materials and Methods

### 3.1 Reagents employed for enzymatic assays

Reagents utilized for buffer preparation were purchased from different suppliers. For instance, sodium citrate (Cat. No. 26300) and citric acid (27915) were purchased from Golden Bell® reagents. Likewise, sodium acetate (Cat. No. A1160), dibasic sodium phosphate (Cat. No. F1330) and monobasic sodium phosphate (Cat. No. F1400) came from Herschi Trading®. As for acetic acid (Cat. No. 320099), glycine (Cat. No. G8898) and tris base (Cat. No. T1503) they were provided by Sigma-Aldrich®. DNS preparation reagents such as potassium sodium tartrate (Cat. No. 3262-19) and sodium bisulfite (Cat. No. 3557) were provided by J.T. Baker® while phenol (Cat. No. F1020) and 3,5-dinitrosalicylic acid (Cat. No. D0550) were purchased from Herschi Trading® and Sigma-Aldrich® respectively. Finally, carbohydrates such as glucose (Cat. No. G5767) and fructose (Cat. No. MFF6-07) were purchased from Sigma-Aldrich® while sucrose (Cat. No. CTR 03772) was obtained from CTR Scientific®.

### 3.2 Strains, plasmids and culture media

*E. coli* BL21 (DE3) from Invitrogen® (Cat. No. 44-0048) was used for culture and production of BfrA. The pD441-CH plasmid, containing a His-tagged *T. maritima* MSB8 BfrA gene, was purchased from ATUM® and used for transformation. SOB agar (yeast extract 0.5% (w/v), tryptone 2% (w/v), NaCl 0.05% (w/v), KCl 0.019% (w/v), 20 mM MgSO<sub>4</sub> and bacteriological agar 1.5% (w/v)) supplemented with 25 µg/mL Kanamycin (SOB agar+Kan) was used for strain transformation confirmation. Recombinant strain maintenance was carried out in SOC agar (yeast extract 0.5% (w/v), tryptone 2% (w/v), NaCl 0.05% (w/v), KCl 0.019% (w/v), glucose 0.36% (w/v) and bacteriological agar 1.5% (w/v)) supplemented with 25 µg/mL Kanamycin (SOC agar+Kan).

On the other hand, LB broth (tryptone 1% (w/v), yeast extract 0.5% (w/v), NaCl 1% (w/v) and glucose 1% (w/v)) supplemented with 25 µg/mL Kanamycin (LB broth+Kan) was employed for BfrA production. All culture media were adjusted to pH 7.0 prior sterilization whilst sterile antibiotic solution was added after. A static microbiological incubator (Novatech®, Model EI60-ED) and a shaking incubator (Labtech®, Model LSI 3016A) were employed for solid and liquid cultures respectively. Temperature and shaking conditions were set to 37°C and 200 rpm respectively.

### 3.3 *E. coli* transformation protocol

200 µL of a vial of *E. coli* BL21 (DE3) was inoculated by spreading over a SOC agar plate and incubated at 37°C for 48 h. Two colonies were picked and used as inoculum for a 250 mL flask with 50 mL of LB broth cultivated overnight at 37 °C and 200 rpm. 2.5 mL of the latter were used as inoculum for a 125 mL flask with 25 mL of LB broth which was then incubated at the same conditions for 4 h. Next, 2 microcentrifuge vials were dispensed with 1 mL of inoculated liquid media and incubated in ice bath at 0 °C for 10 min. Centrifugation of the vials (4000 rpm, 4°C 20°C) was performed in a bench-top centrifuge (Eppendorf®, MniSpin plus) and supernatant was discarded. Cell pellets were resuspended and gently mixed in 1.5 mL of a solution consisting of 80 mM MgCl<sub>2</sub> and 200 mM CaCl<sub>2</sub>. After another centrifugation round (4000 rpm, 4°C 20°C) cell pellets were resuspended and gently mixed in 200 µL of a 0.1 M CaCl<sub>2</sub> solution. Then, 7 µL of pD441-CH plasmid were added to each vial prior a freeze thaw cycle consisting three incubation steps: the first in ice bath at 0 °C for 30 min, the second in water bath at 43 °C for 90 s and the third in ice bath at 0 °C for 2 min. Next, 800 µL of SOC broth were added to each vial and incubated at 37°C and 200 rpm for 45 min. Finally, 200 µL of each vial were inoculated by spreading over SOB+Kan plates and incubated at 37°C. Recombinant *E. coli* colonies grown over the surface of the agar after 24 h of incubation.

### 3.4 Production of recombinant BfrA

Two freshly plated colonies of recombinant *E. coli* were picked and incubated overnight (37 °C and 200 rpm) in a 500 mL flask containing 100 mL of LB broth + Kan. A total of 10 flasks were incubated at the same time. A volume of 0.5 L of overnight culture was used as initial inoculum for a 7.5 L bench top bioreactor loaded with 4.5 L of LB broth + Kan reaching 0.8 OD<sub>600nm</sub> approximately, this procedure was done in duplicate. Batch production of BfrA was controlled by a built-in digital controller (Eppendorf®, New Brunswick BioFlo/CelliGen115, Model BF115-2116354) for pH, temperature, aeration, agitation and DO concentration. Conditions were set at 37°C, pH 7.0 ± 0.5 and ½ vvm while mixing was controlled by an agitation cascade adjusted to 20% DO saturation. After 5 h of cultivation, recombinant BfrA induction was performed through addition of IPTG to a final concentration of 0.4 mM. Batch culture continued for another 3 h before it was stopped. Every hour a 15 mL sample was taken from each bioreactor and centrifuged (3000g, 20 min, 4 °C) in an Eppendorf® 5810R centrifuge. While supernatant was kept stored at 4 °C for residual sugar determination, cell pellet was resuspended in the same volume of dH<sub>2</sub>O and used for dry weight determination.

### 3.5 BfrA purification

A depiction of the process followed can be seen in *Figure 3.1*. Culture broth of both bioreactors were pooled prior centrifugation (40000 rpm, 4°C) in a CEPA® LE tubular centrifuge. Biomass paste was recovered and resuspended in 1 L of LEW buffer (50 mM NaH<sub>2</sub>PO<sub>4</sub>, 300 mM NaCl, pH 8.0) before cell lysis via sonication in a BRANSON® 5510R-DTH ultrasonic bath for 45 mins at room temperature. Cell lysate was centrifuged again (40000 rpm y 4 °C) to recover the soluble fraction, which was filtered through 0.45 µm (Merck®, Cat. No. GSWP04700) and 0.22 µm (Merck®, Cat. No. HVLP04700) pore diameter membranes. Purification of His-tagged recombinant BfrA was carried out via Immobilized Metal Affinity Chromatography (IMAC) in a XK 16/20 column (GE®, Cat. No.

18-8773-01) containing 25 mL of Ni Sepharose 6 FF resin (GE®, Cat. No. 17-5318-01). The column was equilibrated with buffer A (300 mM NaCl, 50 mM NaH<sub>2</sub>PO<sub>4</sub>, 5 mM Imidazole, pH 8.0) at a constant flow rate of 5 mL/min until baseline was reached. Next, 120 mL of filtered soluble fraction was loaded into the column followed by a wash of 8 CV of buffer A. His-tagged protein elution was achieved by a 3 CV step gradient of 100% of buffer B (300 mM NaCl, 50 mM NaH<sub>2</sub>PO<sub>4</sub>, 250 mM Imidazole, pH 8.0). A 10 mL eluted fraction was collected and subjected to dialysis to reduce imidazole content. Briefly, eluted fraction was transferred to a Spectra Por® (Cat. No. 132660) dialysis membrane and subjected to four 1 h washes under stirring. The first with dH<sub>2</sub>O in a ratio of (1:400) and the other three with LEW buffer pH 8.0 in a ratio of (1:100). Dialyzed fraction was stored at -70 °C until further analytical determinations and enzymatic activity assays.

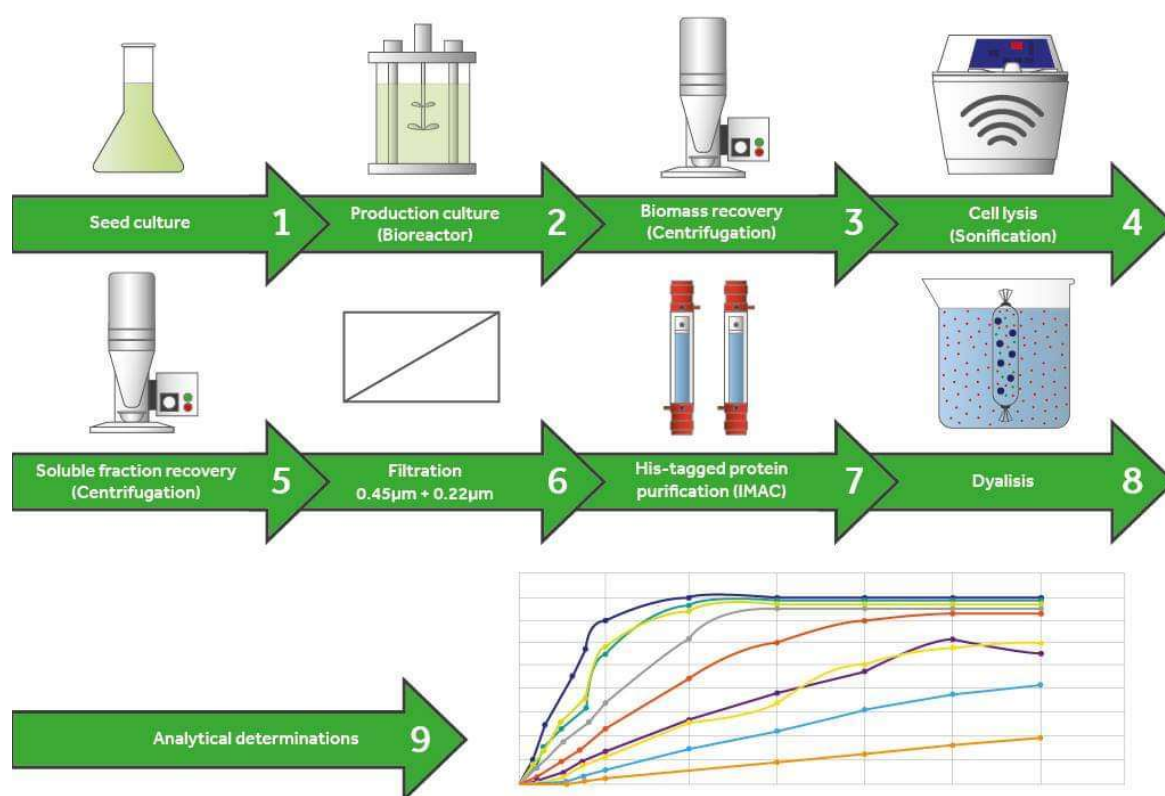


**Figure 3.1** BfrA production and purification train

### 3.6 Analytic methods.

#### *Dry weight determination*

Aluminum trays were stabilized at constant weight by incubating them at 85 °C in a heating oven for 24 h. 5 mL of dH<sub>2</sub>O-washed pellets were poured in an aluminum tray and let dry in the oven for 24 h. Dry weight determinations of each bioreactor were done in duplicate.

#### *Total protein quantification*

Total protein determination of purified fractions of recombinant BfrA from *T. maritima* was assayed using Bradford Reagent from Sigma® (Cat. No. B6916) using manufacturers' protocol with slight modifications. Briefly 200 µL of protein sample was mixed with 1 mL of Bradford reagent at room temperature for 5 minutes. Absorbance readings at 595 nm were performed in a Perkin Elmer® Lambda 25 spectrophotometer using the Perkin Elmer® UV WinLab™ 6.0.3 software. BSA was used for the construction of the calibration curve in an interval between 25 – 125 µg/mL.

#### *Reducing sugar quantification*

Reducing sugars were quantified according to the method of Miller (1959) with some modifications. Briefly, 1 mL of DNS reagent (per litre: 31 mM 3,5 dinitrosalicylic acid, 204 g potassium sodium tartrate, 5.07 mL phenol and 5.53 g Sodium bisulfite) was added to a 1 mL of enzymatic assay mixture or purified sample contained in an assay tube. The latter was incubated in a boiling bath for 5 mins. Tap water was used to cool the mixture followed by the addition of 5 mL of dH<sub>2</sub>O and absorbance readings were done at 550 nm. An equimolar mixture of glucose and fructose was employed for the calibration curve within an interval of 0.1-1 mg/mL.

#### *SDS-PAGE protocol*

Stacking and resolving polyacrylamide gels were prepared according to *Table A.4* (see Appendix C). Once casted, gels were placed in an electrophoresis chamber (BioRad®, Mini-PROTEAN® Tetra Cell)

which was filled with 1X running buffer. Protein samples were prepared by (1:1) dilution with 2X Sample buffer prior a 5 min incubation in boiling bath. Wells were loaded with 20  $\mu$ L of protein sample or 10  $\mu$ L of ECL Rainbow – High Range molecular weight marker (GE®, Cat. No. RPN756E) respectively. For the protein profiling assay (See *Figure 4.2*) lanes 1 to 6 were loaded with 32, 20, 41, 4.5, 15 y 27  $\mu$ g of protein respectively. Electrophoresis run conditions were set to 90V for 2h. Gels were stained with Coomassie blue solution for 3h prior destaining with Destaining solution I for 1h and Destaining solution II overnight. Employed solutions composition can be found in *Table A.5* to *Table A.8* (see Appendix C). Gel imaging, protein detection and densitometry analysis was performed in a BioRad® Gel Doc XR+ System using BioRad® Image lab™ 6.0.1 software respectively.

### 3.7 Enzymatic assays and experimental set-up

#### *Standard enzymatic assay*

Enzymatic activity was determined through initial velocity assays at 75 °C using a Terlab® TE-B160DC water bath. The reaction mixture consisted of sufficiently diluted samples of BfrA in 100 mM Acetate buffer pH 5.50 solution with 120 mM sucrose. At the specified temperature, reaction mixture registered a pH of 5.35 approximately. One international unit (IU) is defined as the amount of enzyme that produces 1  $\mu$ mol of reducing sugar per minute.

#### *Experimental set-up for kinetic parameter determination*

Initial velocity assays at 75 °C, with a fixed enzyme concentration of 8.77 nM, were done shifting pH and sucrose concentration. Reaction mixture (buffer + substrate) pH at 75°C was measured before reaction initiation. A pH interval between 3 to 8 was investigated within eleven levels spaced by 0.5 pH unit each. Different buffer solutions were employed according to the pH required (see *Table 3.1*) , buffer composition is given in *Table A.9* (see Appendix C).

**Table 3.1** Buffers solutions employed at each pH interval

Buffer solution	pH interval
100 mM Citrate buffer	3.50 - 4.00
100 mM Acetate buffer	4.50 - 5.50
100 mM Sodium phosphate buffer	6.00 – 7.50
100 mM Tris-HCl + Gly-NaOH buffer	8.00

Similarly, twelve levels of sucrose concentrations were assayed: 2.92, 5.84, 14.61, 29.22, 146.11, 292.23, 438.34, 584.45, 730.57 1000, 1500 and 2000 mM. Each experimental point was assayed in triplicates following a completely random order

### 3.8 Model fitting and kinetic parameter estimation

Kinetic parameter estimation was done through fitting of equation (18.10) to initial velocity data via Least Square Non-Linear Regression (LSNLR) by iterative algorithms employing Wolfram® Mathematica 11 software. Furthermore, the sum of squared residuals ( $\chi^2$ ), that is, the difference between experimental and estimated velocity values can be expressed as:

$$\chi^2 = \sum [v_0 - v(S, H^+)]^2$$

Where  $v_0$  and  $v$  are the measured and the estimated initial velocities respectively. Noteworthy, the estimated velocity is a function of two variables, namely substrate and hydrogen ion concentration and contains kinetic constants such as  $v_{max}$ ,  $K_m$ , and  $K_i$ . Moreover, given that assays were performed in triplicates following an aleatory order, it is usually a good assumption that experimental errors are random and follow a normal distribution (Cleland, 1967). Then, the fit with the most probable set of kinetic constants is also the one that minimizes  $\chi^2$ .

## Chapter 4. Results and Discussion

### 4.1 BfrA production and purification

Recombinant *E. coli* BL21 strain carrying the gene coding for His-tagged BfrA of *T. maritima* was grown in duplicate in 5L bioreactors cultures for 8 h. As can be observed in *Figure 4.1* a maximum biomass concentration reached 4.5 grams of dry weight per litre whilst glucose was almost depleted after 5 h of culture. It should be noted that this study was centered in BfrA kinetic characterization. Hence, optimization of culture conditions remained outside of the objectives pursued.

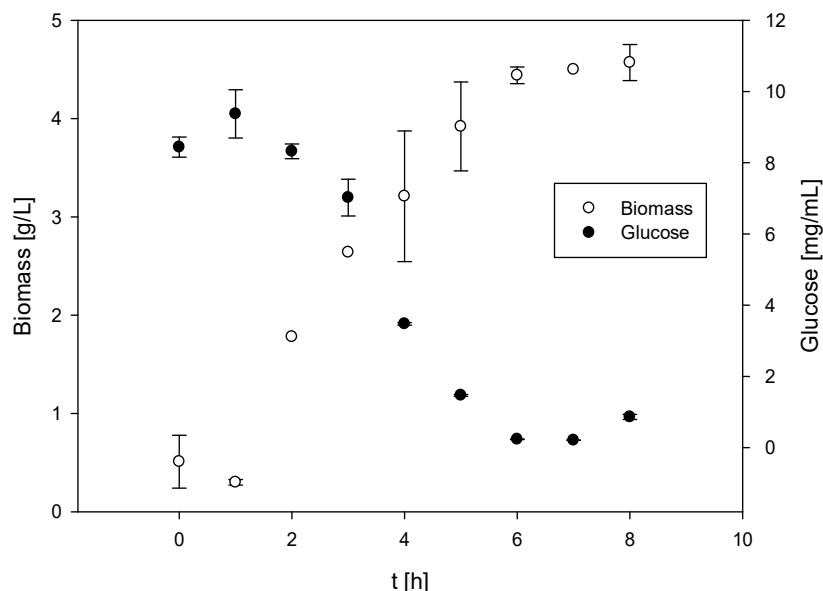


**Figure 4.1** Biomass (dry weight) and glucose profiles for bioreactor culture

Culture broth from both bioreactors were pooled prior biomass recovery through centrifugation. Cellular paste was resuspended in 1 L of LEW buffer before entering cell lysis via sonication. Next, soluble protein fraction from cell lysate was recovered by a second centrifugation step and supernatant was recovered. The latter showed enzymatic activity of 518 UI/mL and 5.05 mg/mL of protein content according to BfrA standard assay and Bradford assay respectively. Further purification steps consisted of filtration, through 0.45 and 0.22  $\mu\text{m}$  pore diameter membranes, and

IMAC chromatography in a column with a Ni Sepharose resin. From a step gradient elution with 250 mM imidazole, a single peak 10 mL of His-tagged protein was recovered (see Appendix, *Figure D.1*). To reduce the imidazole content the latter was dialyzed as described in Materials and Methods. This dialysate showed an enzymatic activity of about 4500 UI/mL and 12.75 mg/mL of protein. The overall yield for the purification methodology was of 77.5% while the highest phase recovery was that of IMAC with 91.9% (see *Table 4.1*).

**Table 4.1** BfrA Purification

	<i>Volume [mL]</i>	<i>Total protein [mg]</i>	<i>Total Activity [UI]</i>	<i>Specific activity [UI/mg]</i>	<i>Purification factor</i>	<i>Overall Yield (%)</i>	<i>Phase Yield (%)</i>
<i>Crude extract (Soluble fraction)</i>	120	607.0	62215.53	102.50	1.0	100.0%	-
<i>Filtration</i>	120	552.0	56574.71	102.49	1.0	90.9%	90.9%
<i>IMAC</i>	10	139.3	52014.14	373.29	3.6	83.6%	91.9%
<i>Dialysis</i>	10.6	135.2	48197.76	356.47	3.5	77.5%	92.7%

Protein profiles of crude extract or soluble fraction, IMAC non-bound fractions and dialysate were determined by SDS-PAGE (See *Figure 4.2*). When comparing to the molecular weight marker in the fifth lane, BfrA can be observed as a band of approximately 50 kDa in both the first and sixth lane, corresponding to soluble and dialyzed fractions respectively. Moreover, several other protein bands, probably host cell proteins from *E. coli* (Pek et al., 2015), are clearly observed in the soluble fraction lane. Many of these bands are observed in the following three lanes, corresponding to non-bound eluted fractions, but no 50 kDa band is seen. In contrast, a more intense 50 kDa corresponding to BfrA is observed in lane 6 along with other faint bands which suggests that most of the enzyme remained bound to chromatography column prior imidazole step gradient elution. Additionally, according to densitometric analysis, BfrA in the dialyzed solution was 81.1% pure.

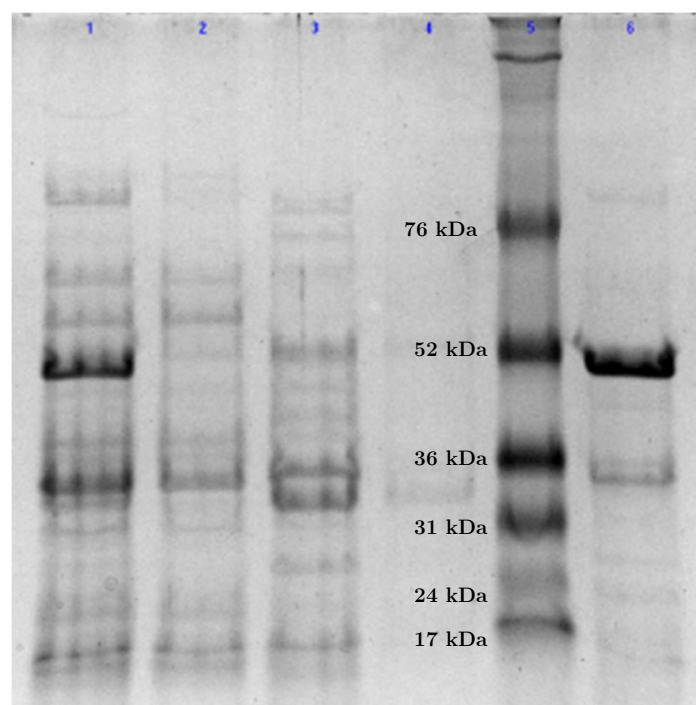


**Figure 4.2** SDS-PAGE from soluble and purified fractions. Lane1: Soluble fraction. Lanes 2-4: Non-bound IMAC fractions. Lane 5: ECL Rainbow – High Range (GE®) molecular weight marker. Lane 6: (Dialyzed) IMAC eluted fraction.

#### 4.2 Determination of BfrA catalytic activity

Progress curves at 75°C were performed in triplicates for each level of substrate concentration and pH in a randomized order. Average progress curves were constructed, and initial velocity was determined by regression of the linear part of the plot (see *Figure 4.3*).

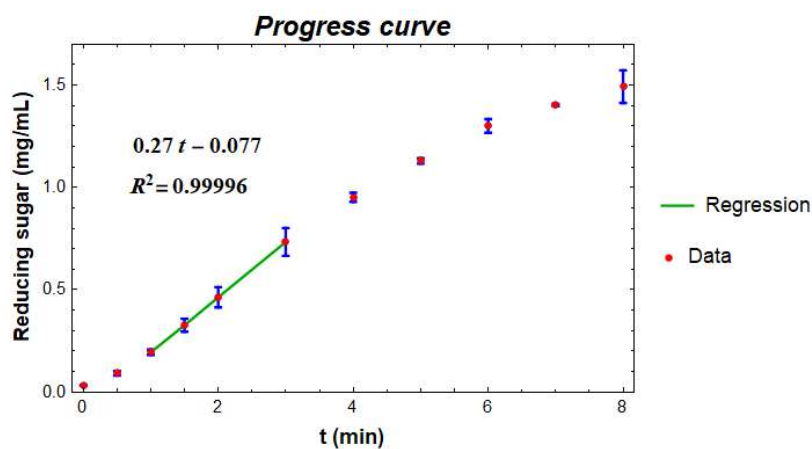


**Figure 4.3** Example progress curve 146.11 mM sucrose and pH 5.56

Plots of initial velocities against substrate at fixed pH (after pH 4.5) showed that the prior increased proportionally with sucrose concentration until 146-292 mM and then started to decrease (see *Figure 4.4 A*). This pattern is characteristic of uncompetitive substrate inhibition and has been reported previously for *T. maritima* BfrA (Liebl et al., 1998; Menéndez et al., 2013). Even though the exact mechanism behind substrate inhibition in BfrA is not yet fully understood, some authors have proposed that reduced water activity conditions, substrate agglomeration and even substrate-mediated electrostatic regulation of catalytic amino acids are likely to be implicated (Bowski et al., 1971; Combes & Monsan, 1983; Yuan et al., 2012).

On the other hand, when plotting initial velocities against pH at fixed substrate concentrations, the maximum values for the prior were found between 4.5 and 5.5. However, drastic differences in enzymatic activity could be seen at pH values of 4.0 and 6.0 which coincides with the change of buffer solution (see *Figure 4.4 B*). Although enzymatic activity decrease is usually linked solely to the change in medium pH, buffer composition might have some influence in regard of differences in ionic force. For instance, Menéndez et al. (2013) observed lower activity of *T. maritima* BfrA at pH 6.0 when employing phosphate buffer instead of acetate buffer. Similar behavior has been reported previously for other glycoside hydrolases such as fungal  $\beta$ -glucosidases (Kudo et al., 2015), wheat-derived  $\beta$ -amylase (Ballou & Luck, 1941) and invertase from soil samples (Vaughan & Malcolm, 1984).

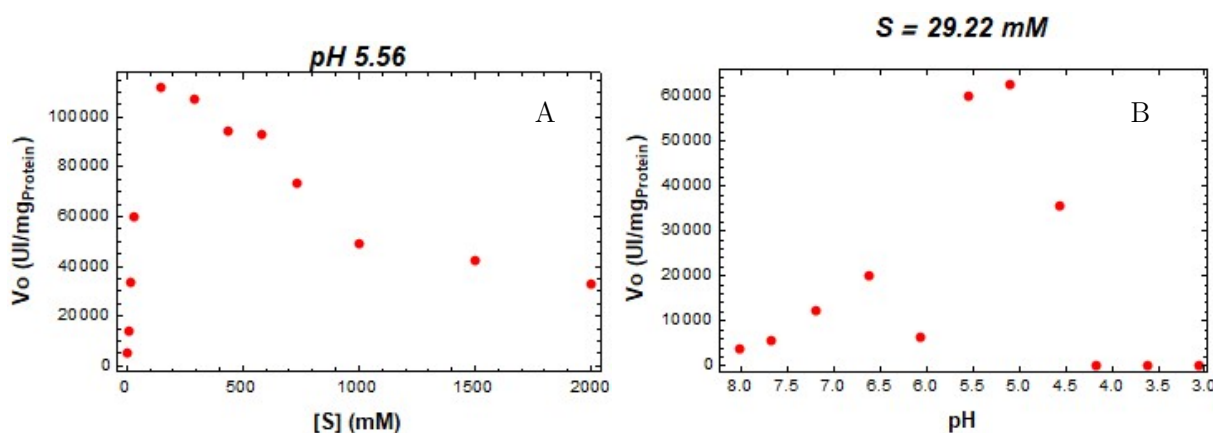


**Figure 4.4** Example plots of initial velocity against substrate (A) and pH (B)

### 4.3 BfrA activity modelling

Initial velocity data was used to fit the proposed model through LSNLR by two different approaches: with varying substrate concentration at fixed pH and varying both pH and substrate. Even though graphical methodologies (i.e. plots of linearized versions of velocity equations) are still widely employed today for velocity equation fitting and parameter estimation, they carry drawbacks such as increased error at low substrate concentrations as well as no estimation on reliability of fitted kinetic constants (Al-Haque et al., 2012; Cleland, 1967; Johnson, 2013). Besides, since the velocity equation (18.10) contains a quadratic term of  $[S]$  and strays away from the regular Michaelis-Menten form, straightforward graphical analysis became complicated. Therefore, non-linear regression was chosen as a more suited methodology for velocity equation fitting and parameter estimation.

In order to establish some delimitations for the model, values for ionization constants ( $K_v$ ) were bound to those of ionizable groups of amino acids involved in BfrA catalysis, namely aspartic and glutamic acid (Alberto et al., 2004). Reported  $pK_a$  values for the side-chain carboxylic groups of these amino acids are between 3.0 and 5.0 (see *Table 4.2*).

**Table 4.2** Ionizable groups and their corresponding amino acid that could be present at the catalytic site.  
Modified from (Segel, 1975)

Amino acid	Ionization group	$pK_a$
C-terminal	Carboxyl	3.0 – 3.4
Aspartic acid or Glutamic acid	Carboxyl	3.0 – 5.0
Histidine	Imidazole	5.5 – 7.0
N-terminal	Ammonium	7.5 – 8.5
Cysteine	Thiol	8.0 – 8.5
Tyrosine	Phenol	9.8 – 10.5
Lysine	Ammonium	9.5 – 10.6
Arginine	Guanidium	11.6 – 12.6

In the first approach, the model showed good adjustment with respect of experimental data at most of the pH values evaluated. However, poor fitting was observed at acidic values of 4.0 or lower (see Appendix E). Nevertheless, from pH 4.5 and onwards, the model readily described enzyme's catalytic behavior, including the effects of substrate inhibition (see *Figure 4.5*).

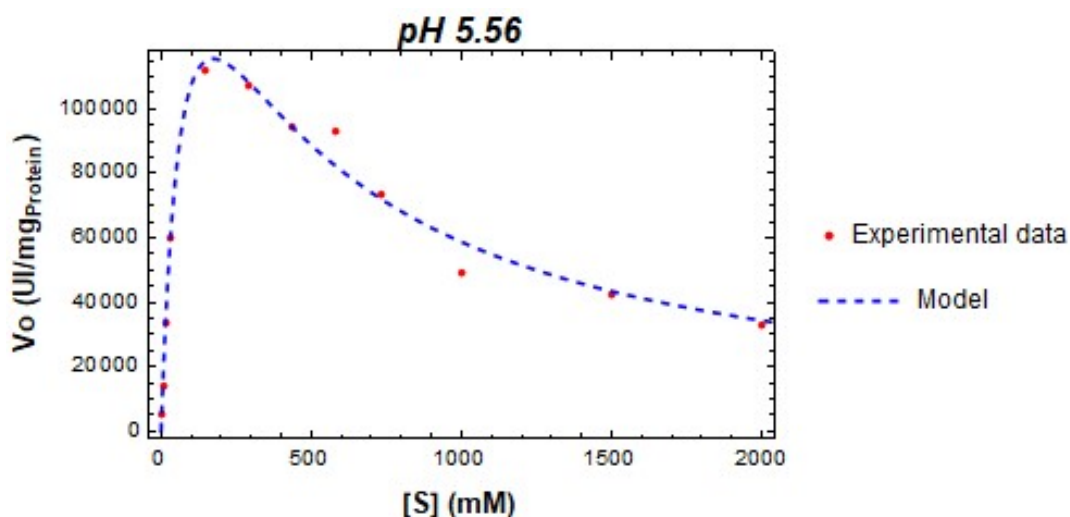


**Figure 4.5** Plot of initial activity vs substrate concentration

Then, the model was fitted for the conditions of the second approach using a two-variable LSNLR to obtain a surface of response. In contrast, this time the model showed poor fitting with respect to experimental data (see *Figure 4.6*). The latter became apparent given the increase in its least squares sum (see *Table 4.3* and *Table 4.5*). Even though experimental data showed a tendency to form a bell-shape like form with a maximum around 4.5 and 5.5, the model narrowed it between 4.5 and 5.0. Moreover, after pH 6.0 the model seemed to lose sensitivity as no change in velocity was noticeable at substrate concentration of 500 mM or higher.

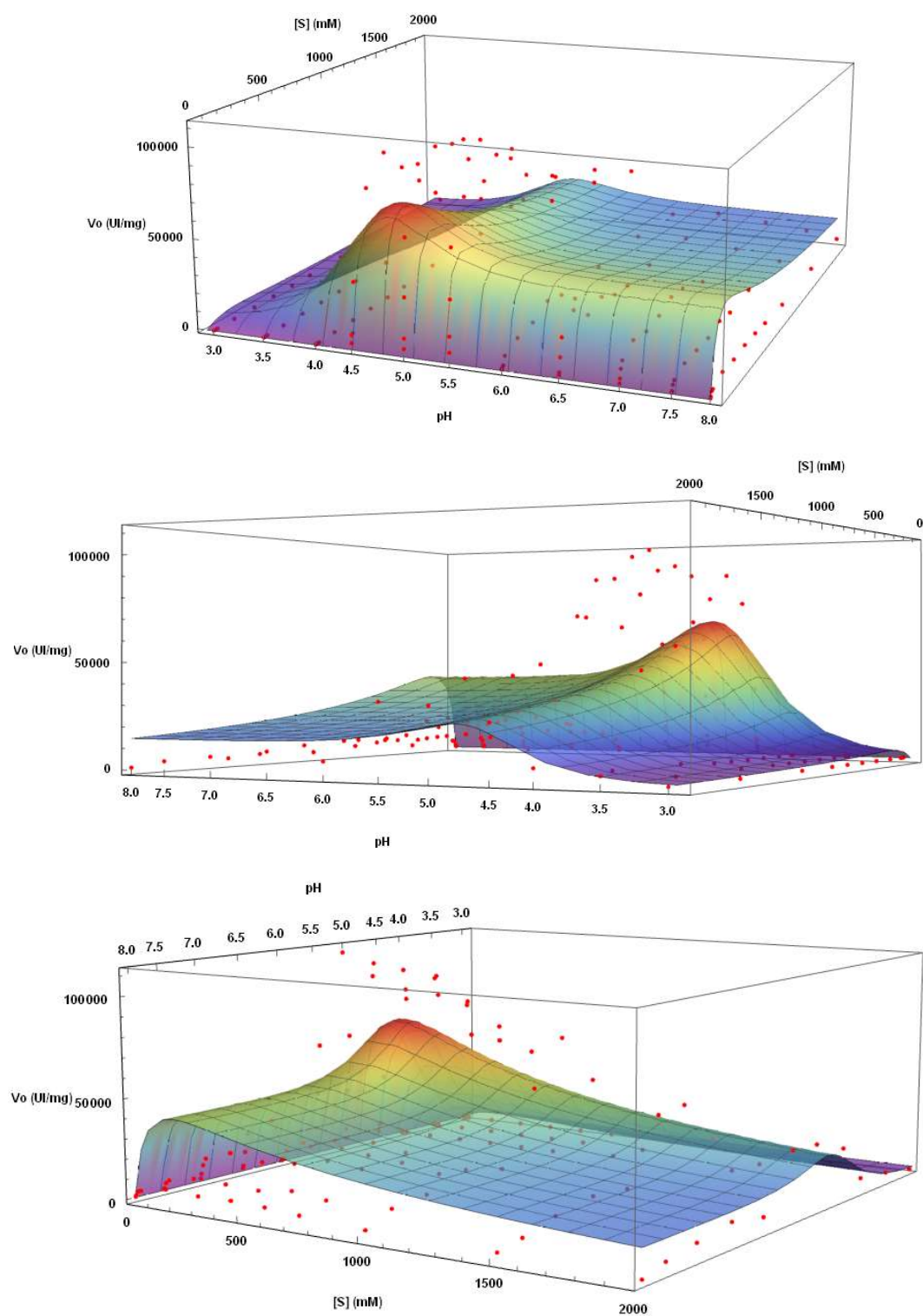


Figure 4.6 Surface of response (1<sup>st</sup> model) and experimental data points (red dots)

Aiming to find some insight about the models' lack of fit, an in-depth search of the currently available literature was conducted. Thereafter, it was found that side-chain carboxylic groups of amino acids that serve as general acid/base in glycoside hydrolases usually display abnormally high  $pK_a$  values (Søndergaard et al., 2008). Particularly for *T. maritima* BfrA, Glu  $pK_a$  has been reported to be around 6.5 (Yuan et al., 2012). With this new information, the model was evaluated once again modifying the limits for the ionization constants involved in catalysis.

This change in limits resulted in enhanced sensitivity and velocity prediction at both acidic and alkaline branches which in turn reduced the sum of squared residuals for the 2<sup>nd</sup> model in the second approach (see *Figure 4.7*, *Table 4.4* and *Table 4.5*). Likewise, the maximum activity interval was broadened to the values suggested by experimental data (i.e. between 4.5 and 5.5). This fitting improvement can be further understood if we analyze BfrA catalytic mechanism. Since Asp and Glu work as nucleophile and general acid/base respectively, the prior must be negatively charged while the latter should shift easily from a protonated to a deprotonated form (Harris & Turner, 2002). This condition is only met when medium pH is above Asp  $pK_a$  and near to that of Glu and, as hinted by experimental data, this is more likely to happen around 4.5 and 5.5. Since the 1<sup>st</sup> model estimated catalytic ionization constants between 3.0 and 5.0, maximum activity interval was reduced.

Despite the 2<sup>nd</sup> model's good results for the second approach, lack of fit at pH between 3.0 and 4.0 did not change for the first approach. This can be attributed to negligible activity measurements at most of the sucrose concentrations evaluated (see Appendix E). Drastic reduction in catalytic potential at acidic pH is likely due to enzyme denaturation which has been reported to be more pronounced in non-glycosylated forms of *S. cerevisiae* BfrA (Kern et al., 1992) and other glycoside hydrolases (Barroca et al., 2017; Kudo et al., 2015). Additionally, some authors have reported spectrophotometric quantification methods sensitivity at acidic pH (Garriga et al., 2017; Herrera et

al., 2008). Considering the previous information, results obtained between pH 3.0 and 4.0 were not further considered for neither data analysis nor kinetic parameter estimation in the first approach.

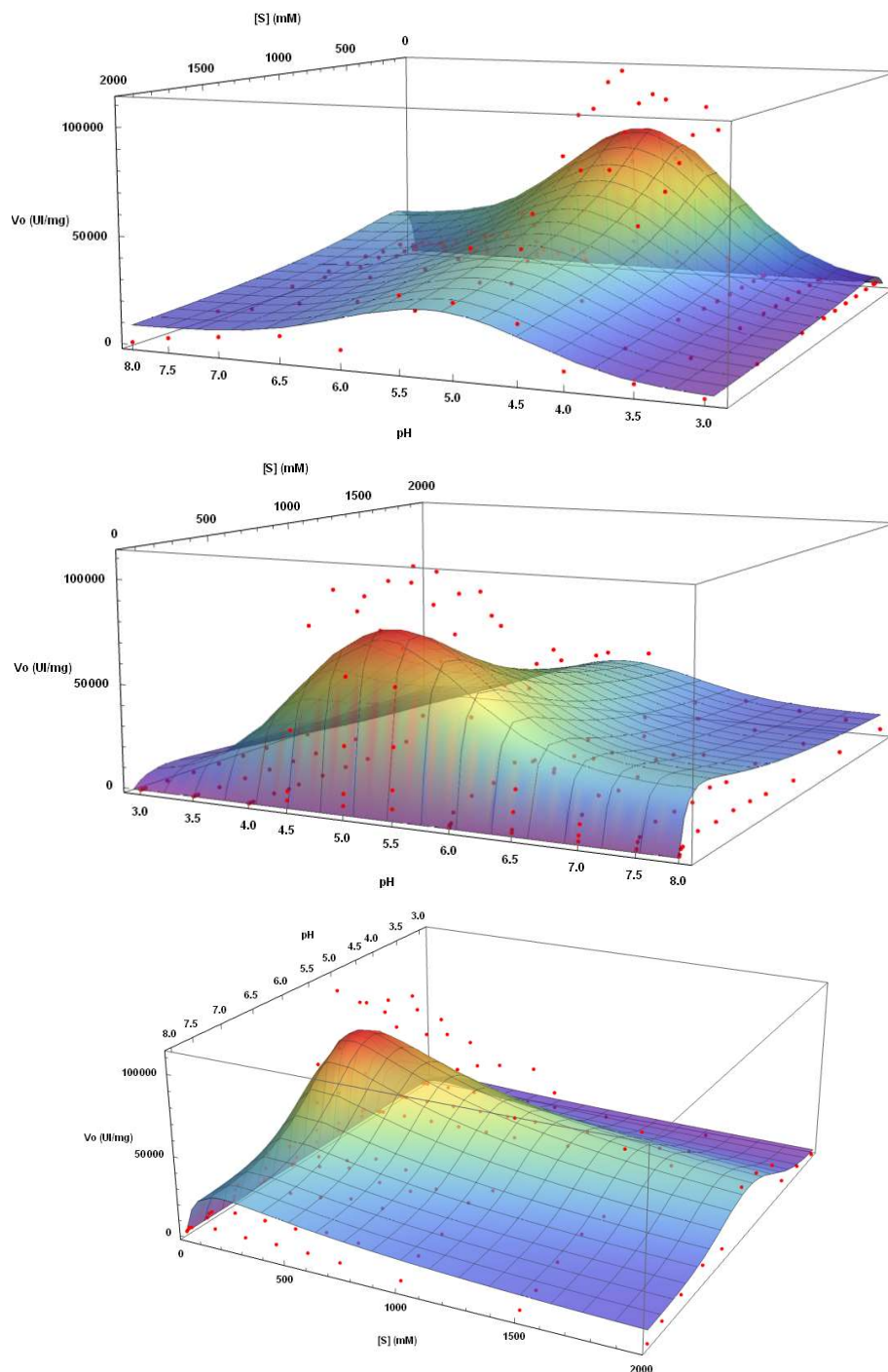


**Figure 4.7** Surface of response (2<sup>nd</sup> model) and experimental data points (red dots)

#### 4.4 BfrA kinetic characterization

Two sets of parameters, corresponding to each approach, were estimated for each model along with their standard deviation. Since the first approach was applied at different levels of fixed pH, an equal number of parameter series and least squares sums were obtained (see *Table 4.3* and *Table 4.4*). For the second approach, however, only a single series of parameters and least squares sum were obtained per model evaluated (see *Table 4.5*).

**Table 4.3** Estimated kinetic parameters (1<sup>st</sup> model, 1<sup>st</sup> approach) and sum of squared residuals ( $\chi^2$ )

	pH							
	4.56	5.10	5.56	6.08	6.63	7.20	7.68	8.03
$v_{max}^a$	$3.40 \times 10^5 \pm$	$2.80 \times 10^5 \pm$	$3.28 \times 10^5 \pm$	$2.69 \times 10^5 \pm$	$1.21 \times 10^5 \pm$	$1.58 \times 10^5 \pm$	$1.67 \times 10^5 \pm$	$1.37 \times 10^5 \pm$
	$1.86 \times 10^{-8} *$	$3.69 \times 10^{-8} *$	$2.31 \times 10^{-8} *$	$4.00 \times 10^{-9} *$	$2.11 \times 10^{-8} *$	$1.15 \times 10^{-8} *$	$2.22 \times 10^{-9} *$	$2.78 \times 10^{-9} *$
$K_m^b$	$62.62 \pm$	$64.49 \pm$	$62.51 \pm$	$62.59 \pm$	$61.94 \pm$	$62.49 \pm$	$62.48 \pm$	$62.49 \pm$
	$1.07 \times 10^{-3} *$	$9.77 \times 10^{-4} *$	$8.11 \times 10^{-4} *$	$6.43 \times 10^{-3} *$	$6.32 \times 10^{-4} *$	$1.74 \times 10^{-3} *$	$1.41 \times 10^{-3} *$	$1.20 \times 10^{-3} *$
$K_i^b$	$571.16 \pm$	$709.33 \pm$	$581.93 \pm$	$621.66 \pm$	$539.11 \pm$	$610.09 \pm$	$621.04 \pm$	$555.64 \pm$
	$1.01 \times 10^{-4} *$	$1.10 \times 10^{-4} *$	$8.91 \times 10^{-5} *$	$1.20 \times 10^{-2} *$	$1.46 \times 10^{-4} *$	$1.75 \times 10^{-4} *$	$8.21 \times 10^{-5} *$	$2.55 \times 10^{-4} *$
$K_{el}^b$	$4.17 \times 10^{-1} \pm$	$4.51 \times 10^{-1} \pm$	$4.26 \times 10^{-1} \pm$	$4.26 \times 10^{-1} \pm$	$3.62 \times 10^{-1} \pm$	$4.26 \times 10^{-1} \pm$	$4.26 \times 10^{-1} \pm$	$4.26 \times 10^{-1} \pm$
	$4.16 \times 10^{-4} *$	$4.77 \times 10^{-5} *$	$4.62 \times 10^{-6} *$	$2.45 \times 10^{-6} *$	$6.95 \times 10^{-8} *$	$7.33 \times 10^{-9} *$	$6.69 \times 10^{-10} *$	$1.00 \times 10^{-10} *$
$K_{e2}^b$	$6.77 \times 10^{-1} \pm$	$4.01 \times 10^{-1} \pm$	$4.57 \times 10^{-1} \pm$	$6.25 \times 10^{-1} \pm$	$2.36 \times 10^{-1} \pm$	$3.27 \times 10^{-1} \pm$	$3.17 \times 10^{-1} \pm$	$3.58 \times 10^{-1} \pm$
	$9.53 \times 10^{-2}$	$1.54 \times 10^{-1}$	$1.10 \times 10^{-1}$	$6.43 \times 10^{-1}$	$1.66 \times 10^{-1}$	$3.33 \times 10^{-1}$	$2.78 \times 10^{-1}$	$2.09 \times 10^{-1}$
$K_{es1}^b$	$4.30 \times 10^{-1} \pm$	$4.51 \times 10^{-1} \pm$	$4.26 \times 10^{-1} \pm$	$4.26 \times 10^{-1} \pm$	$3.62 \times 10^{-1} \pm$	$4.26 \times 10^{-1} \pm$	$4.26 \times 10^{-1} \pm$	$4.26 \times 10^{-1} \pm$
	$8.33 \times 10^{-4} *$	$6.61 \times 10^{-5} *$	$6.95 \times 10^{-6} *$	$3.27 \times 10^{-6} *$	$9.18 \times 10^{-8} *$	$6.41 \times 10^{-9} *$	$4.44 \times 10^{-10} *$	$1.69 \times 10^{-10} *$
$K_{es2}^b$	$2.53 \times 10^{-2} \pm$	$4.22 \times 10^{-1} \pm$	$3.39 \times 10^{-1} \pm$	$4.87 \times 10^{-1} \pm$	$4.57 \times 10^{-1} \pm$	$6.23 \times 10^{-1} \pm$	$6.53 \times 10^{-1} \pm$	$4.77 \times 10^{-1} \pm$
	$2.03 \times 10^{-1}$	$2.13 \times 10^{-1}$	$1.66 \times 10^{-1}$	$8.55 \times 10^{-1}$	$2.19 \times 10^{-1}$	$2.92 \times 10^{-1}$	$1.18 \times 10^{-1}$	$3.51 \times 10^{-1}$
$K_{vl}^b$	$4.30 \times 10^{-1} \pm$	$4.55 \times 10^{-1} \pm$	$4.31 \times 10^{-1} \pm$	$4.31 \times 10^{-1} \pm$	$3.68 \times 10^{-1} \pm$	$4.31 \times 10^{-1} \pm$	$4.31 \times 10^{-1} \pm$	$4.31 \times 10^{-1} \pm$
	$2.13 \times 10^{-4} *$	$1.18 \times 10^{-5} *$	$1.31 \times 10^{-6} *$	$1.16 \times 10^{-7} *$	$7.41 \times 10^{-9} *$	$4.11 \times 10^{-10} *$	$1.98 \times 10^{-11} *$	$3.75 \times 10^{-12} *$
$K_{v2}^b$	$9.26 \times 10^{-2} \pm$	$2.58 \times 10^{-1} \pm$	$2.34 \times 10^{-1} \pm$	$3.37 \times 10^{-2} \pm$	$1.40 \times 10^{-1} \pm$	$9.53 \times 10^{-2} \pm$	$4.40 \times 10^{-2} \pm$	$3.92 \times 10^{-2} \pm$
	$5.18 \times 10^{-2}$	$3.89 \times 10^{-2}$	$3.19 \times 10^{-2}$	$3.12 \times 10^{-2}$	$1.83 \times 10^{-2}$	$1.91 \times 10^{-2}$	$8.40 \times 10^{-3}$	$7.99 \times 10^{-3}$
$K_{ess1}^b$	$4.21 \times 10^{-1} \pm$	$4.51 \times 10^{-1} \pm$	$4.25 \times 10^{-1} \pm$	$4.26 \times 10^{-1} \pm$	$3.62 \times 10^{-1} \pm$	$4.26 \times 10^{-1} \pm$	$4.26 \times 10^{-1} \pm$	$4.26 \times 10^{-1} \pm$
	$5.33 \times 10^{-2} *$	$4.63 \times 10^{-5} *$	$3.92 \times 10^{-6} *$	$1.37 \times 10^{-6} *$	$9.16 \times 10^{-8} *$	$7.50 \times 10^{-9} *$	$5.69 \times 10^{-10} *$	$1.15 \times 10^{-10} *$
$K_{ess2}^b$	$4.37 \times 10^{-1} \pm$	$5.14 \times 10^{-1} \pm$	$5.52 \times 10^{-1} \pm$	$2.07 \times 10^{-1} \pm$	$3.60 \times 10^{-1} \pm$	$3.12 \times 10^{-1} \pm$	$2.16 \times 10^{-1} \pm$	$5.93 \times 10^{-1} \pm$
	$1.24 \times 10^{-1}$	$1.49 \times 10^{-1}$	$9.36 \times 10^{-2}$	$3.58 \times 10^{-1}$	$2.18 \times 10^{-1}$	$3.41 \times 10^{-1}$	$2.63 \times 10^{-1}$	$2.39 \times 10^{-1}$
$\chi^2$	$2.60 \times 10^8$	$4.01 \times 10^8$	$2.40 \times 10^8$	$7.53 \times 10^7$	$6.23 \times 10^7$	$5.47 \times 10^7$	$1.02 \times 10^7$	$3.79 \times 10^6$

(\*)  $p < 0.05$ . (a) UI/mg. (b) mM

**Table 4.4** Estimated kinetic parameters (2<sup>nd</sup> model, 1<sup>st</sup> approach) and sum of squared residuals ( $\chi^2$ )

	pH							
	4.56	5.10	5.56	6.08	6.63	7.20	7.68	8.03
$v_{max}^a$	1.50x10 <sup>5</sup> ± 1.35x10 <sup>-9</sup> *	1.93x10 <sup>5</sup> ± 5.43x10 <sup>-11</sup> *	2.35x10 <sup>5</sup> ± 5.66x10 <sup>-12</sup> *	3.49x10 <sup>4</sup> ± 4.64x10 <sup>-11</sup> *	1.14x10 <sup>5</sup> ± 7.29x10 <sup>-13</sup> *	9.90x10 <sup>4</sup> ± 6.68x10 <sup>-13</sup> *	5.14x10 <sup>4</sup> ± 1.00x10 <sup>-12</sup> *	3.79x10 <sup>4</sup> ± 1.39x10 <sup>-12</sup> *
$K_m^b$	65.00± 1.15x10 <sup>-5</sup> *	62.48± 5.51x10 <sup>-7</sup> *	62.57± 8.55x10 <sup>-8</sup> *	62.67± 1.93x10 <sup>-7</sup> *	62.47± 1.65x10 <sup>-8</sup> *	62.48± 2.56x10 <sup>-8</sup> *	62.48± 1.92x10 <sup>-8</sup> *	62.48± 1.57x10 <sup>-8</sup> *
$K_i^b$	505.59± 1.03x10 <sup>-6</sup> *	581.46± 5.28x10 <sup>-8</sup> *	510.08± 9.22x10 <sup>-9</sup> *	673.52± 3.59x10 <sup>-9</sup> *	586.89± 4.09x10 <sup>-9</sup> *	614.80± 2.57x10 <sup>-9</sup> *	622.00± 1.12x10 <sup>-9</sup> *	560.87± 3.36x10 <sup>-9</sup> *
$K_{el}^b$	0.32± 1.71x10 <sup>-4</sup> *	5.00± 9.16x10 <sup>-9</sup> *	5.00± 3.47x10 <sup>-10</sup> *	5.00± 1.01x10 <sup>-10</sup> *	5.00± 1.85x10 <sup>-12</sup> *	5.00± 2.03x10 <sup>-13</sup> *	5.00± 1.79x10 <sup>-14</sup> *	5.00± 2.64x10 <sup>-15</sup> *
$K_{e2}^b$	3.16x10 <sup>-3</sup> ± 2.25x10 <sup>-2</sup>	1.52x10 <sup>-3</sup> ± 3.63x10 <sup>-4</sup>	1.93x10 <sup>-3</sup> ± 1.14x10 <sup>-3</sup>	2.48x10 <sup>-3</sup> ± 3.66x10 <sup>-3</sup>	9.86x10 <sup>-4</sup> ± 8.45x10 <sup>-4</sup>	1.19x10 <sup>-3</sup> ± 1.28x10 <sup>-3</sup>	1.15x10 <sup>-3</sup> ± 1.02x10 <sup>-3</sup>	1.28x10 <sup>-3</sup> ± 7.57x10 <sup>-4</sup>
$K_{es1}^b$	6.31± 5.24x10 <sup>-7</sup> *	5.00± 1.11x10 <sup>-8</sup> *	5.01± 4.90x10 <sup>-10</sup> *	5.00± 1.20x10 <sup>-10</sup> *	5.00± 2.66x10 <sup>-12</sup> *	5.00± 1.79x10 <sup>-13</sup> *	5.00± 1.20x10 <sup>-14</sup> *	5.00± 4.41x10 <sup>-15</sup> *
$K_{es2}^b$	1.58x10 <sup>-3</sup> ± 2.75x10 <sup>-2</sup>	1.68x10 <sup>-3</sup> ± 4.42x10 <sup>-3</sup>	7.27x10 <sup>-4</sup> ± 1.62x10 <sup>-3</sup>	1.75x10 <sup>-3</sup> ± 4.36x10 <sup>-3</sup>	2.15x10 <sup>-3</sup> ± 1.21x10 <sup>-3</sup>	2.33x10 <sup>-3</sup> ± 1.12x10 <sup>-3</sup>	2.39x10 <sup>-3</sup> ± 6.86x10 <sup>-4</sup>	1.71x10 <sup>-3</sup> ± 1.27x10 <sup>-3</sup>
$K_{v1}^b$	5.58x10 <sup>-1</sup> ± 1.67x10 <sup>-5</sup> *	5.52x10 <sup>-1</sup> ± 2.08x10 <sup>-7</sup> *	5.51x10 <sup>-1</sup> ± 9.85x10 <sup>-9</sup> *	5.50x10 <sup>-1</sup> ± 2.63x10 <sup>-9</sup> *	5.50x10 <sup>-1</sup> ± 1.94x10 <sup>-11</sup> *	5.50x10 <sup>-1</sup> ± 1.49x10 <sup>-12</sup> *	5.50x10 <sup>-1</sup> ± 1.41x10 <sup>-13</sup> *	5.50x10 <sup>-1</sup> ± 2.97x10 <sup>-14</sup> *
$K_{v2}^b$	6.23x10 <sup>-4</sup> ± 6.84x10 <sup>-3</sup>	6.18x10 <sup>-4</sup> ± 1.00x10 <sup>-3</sup>	6.08x10 <sup>-4</sup> ± 3.94x10 <sup>-4</sup>	5.76x10 <sup>-4</sup> ± 1.15x10 <sup>-3</sup>	5.44x10 <sup>-4</sup> ± 1.07x10 <sup>-4</sup>	5.20x10 <sup>-4</sup> ± 1.13x10 <sup>-4</sup>	5.07x10 <sup>-4</sup> ± 9.76x10 <sup>-5</sup>	5.03x10 <sup>-4</sup> ± 1.03x10 <sup>-4</sup>
$K_{ess1}^b$	4.96± 5.46x10 <sup>-7</sup> *	5.00± 8.07x10 <sup>-9</sup> *	5.00± 2.88x10 <sup>-10</sup> *	5.00± 5.59x10 <sup>-11</sup> *	5.00± 2.58x10 <sup>-12</sup> *	5.00± 2.09x10 <sup>-13</sup> *	5.00± 1.52x10 <sup>-14</sup> *	5.00± 3.04x10 <sup>-15</sup> *
$K_{ess2}^b$	1.71x10 <sup>-3</sup> ± 1.77x10 <sup>-2</sup>	1.65x10 <sup>-3</sup> ± 3.20x10 <sup>-3</sup>	2.20x10 <sup>-3</sup> ± 9.50x10 <sup>-4</sup>	3.63x10 <sup>-4</sup> ± 2.02x10 <sup>-3</sup>	1.81x10 <sup>-3</sup> ± 1.17x10 <sup>-3</sup>	1.14x10 <sup>-3</sup> ± 1.31x10 <sup>-3</sup>	7.77x10 <sup>-4</sup> ± 8.70x10 <sup>-4</sup>	2.15x10 <sup>-3</sup> ± 8.72x10 <sup>-4</sup>
$\chi^2$	8.78x10 <sup>8</sup>	4.01x10 <sup>8</sup>	2.40x10 <sup>8</sup>	7.53x10 <sup>7</sup>	6.23x10 <sup>7</sup>	5.47x10 <sup>7</sup>	1.02x10 <sup>7</sup>	3.79x10 <sup>6</sup>

(\*)  $p < 0.05$ . (a) UI/mg. (b) mM

In the first approach all kinetic constants (i.e.  $v_{max}$ ,  $K_m$  and  $K_i$ ) had a significance value of  $p < 0.05$  (see Table 4.2). It was observed that  $K_m$  and  $K_i$  varied slightly between 61-66 mM and 500-700 mM respectively. On the contrary,  $v_{max}$  was quite sensitive to pH changes as it oscillated between 1.21x10<sup>5</sup> - 3.40x10<sup>5</sup> UI/mg for the 1<sup>st</sup> model and between 3.49x10<sup>4</sup> - 2.35x10<sup>5</sup> UI/mg for the 2<sup>nd</sup>. While similar  $K_m$  values have been reported earlier for *T. maritima* BfrA, comparison of  $K_i$  became difficult since previous studies worked solely under non-inhibition conditions (Liebl et al., 1998; Menéndez et al., 2013). Despite BfrA substrate inhibition has been acknowledged extensively, only few works with the enzyme from *S. cerevisiae* have estimated kinetic parameters at high substrate concentrations (Bowski et al., 1971; Combes & Monsan, 1983) and only one reported a  $K_i$  of 473 mM (Keramat et

al., 2017). On the other hand, while acidic ionizations constants estimation was accurate for both models, estimated alkaline constants had big standard deviations. However, estimates provided by the 2<sup>nd</sup> model were not as dissimilar as those from the 1<sup>st</sup> model.

Then, by substituting estimated parameters in equations (29), (30) and (31), apparent kinetic constants (i.e.  $v_{max}^{app}$ ,  $K_m^{app}$  and  $K_i^{app}$ ) were determined for each value of pH and logarithmic plots were obtained (see *Figure 4.8*). Despite of the differences in parameter estimation between the models, apparent kinetic constants remained almost the same. Similar to the above-mentioned results,  $v_{max}^{app}$  exhibited its highest value around pH 4.5 and 5.5. On the other hand,  $K_m^{app}$  showed an inverse relationship with increasing pH whilst  $K_i^{app}$  increased only slightly. Regardless of the effect of alkaline conditions over substrate affinity and inhibition, catalytic activity was greatly reduced above pH 6.0.

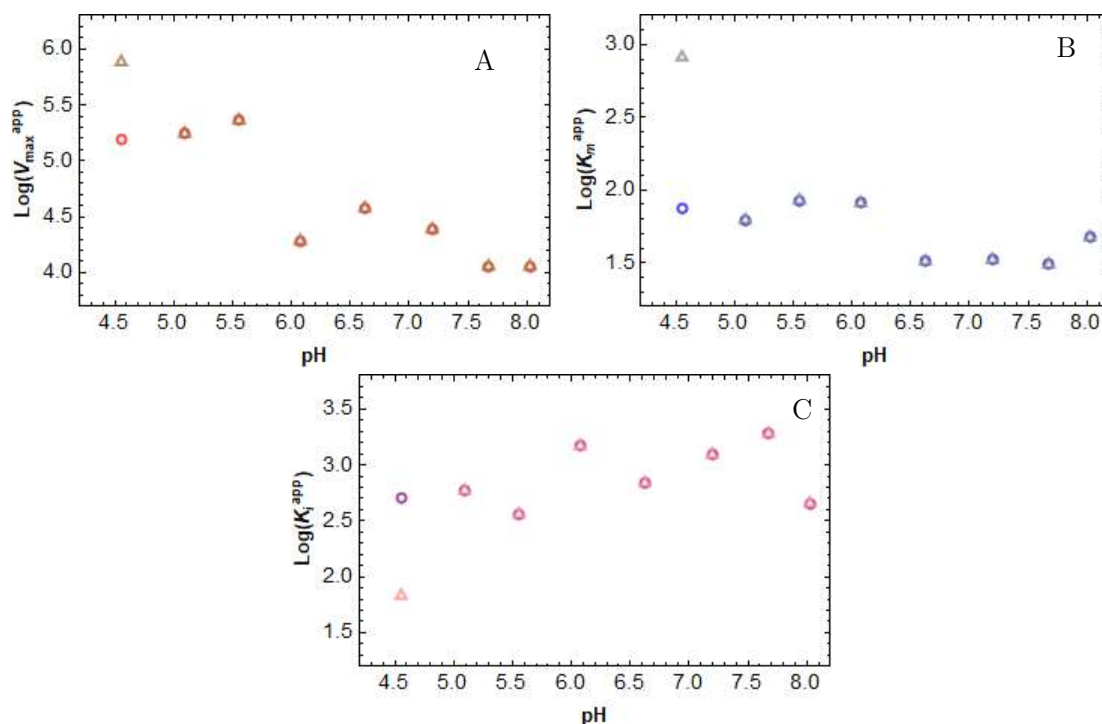


**Figure 4.8** Apparent kinetic parameters against pH for the 1<sup>st</sup> (triangles) and 2<sup>nd</sup> (circles) model

Regardless of the model, estimated parameters in the second approach obtained a significance value of  $p > 0.05$ . However, standard deviations for parameters obtained in the 2<sup>nd</sup> model were much smaller in comparison to those of the 1<sup>st</sup> model. Moreover, the 2<sup>nd</sup> model provided the set of parameters that reduced the least squares sum the most, hence, providing a better fit than the 1<sup>st</sup> model.

**Table 4.5** Estimated kinetic parameters (2<sup>nd</sup> approach) and sum of squared residuals ( $\chi^2$ )

	1 <sup>st</sup> model	2 <sup>nd</sup> model		1 <sup>st</sup> model	2 <sup>nd</sup> model
$v_{max}^a$	$2.00 \times 10^5 \pm 7.535 \times 10^7$	$1.80 \times 10^5 \pm 1.12 \times 10^5$	$K_{el}^b$	$5.88 \times 10^{-4} \pm 5.17 \times 10^{-2}$	$2.04 \times 10^{-2} \pm 3.61 \times 10^{-2}$
$K_m^b$	$40.00 \pm 4.27 \times 10^3$	$68.41 \pm 86.12$	$K_{e2}^b$	$4.61 \times 10^{-1} \pm 40.20$	$1.00 \times 10^{-3} \pm 1.47 \times 10^{-3}$
$K_i^b$	$900.00 \pm 7.75 \times 10^4$	$499.75 \pm 552.434$	$K_{ess1}^b$	$3.79 \times 10^{-3} \pm 1.57 \times 10^{-1}$	$5.89 \times 10^{-2} \pm 1.61 \times 10^{-1}$
$\chi^2$	$4.34 \times 10^8$	$2.99 \times 10^8$	$K_{ess2}^b$	$2.81 \times 10^{-1} \pm 10.80$	$1.00 \times 10^{-3} \pm 1.25 \times 10^{-3}$
			$K_{v1}^b$	$8.51 \times 10^{-1} \pm 4.07$	$1.00 \pm 2.58$
			$K_{v2}^b$	$1.00 \times 10^{-2} \pm 1.46 \times 10^{-2}$	$2.51 \times 10^{-4} \pm 1.75 \times 10^{-4}$
			$K_{ess1}^b$	$8.01 \times 10^{-4} \pm 5.25 \times 10^{-2}$	$2.84 \times 10^{-2} \pm 4.02 \times 10^{-2}$
			$K_{ess2}^b$	$4.81 \times 10^{-1} \pm 31.30$	$1.00 \times 10^{-3} \pm 1.18 \times 10^{-3}$

(a) UI/mg, (b) mM

To acquire a better understanding of the influence of pH over BfrA, further analysis of ionization constants was performed. Considering the previous results, only the 2<sup>nd</sup> model was contemplated for calculation of  $pK_a$  values for ionizable groups theoretically involved in catalysis ( $pK_v$ ), substrate binding ( $pK_{es}$ ) and inhibition ( $pK_{ess}$ ). While acid and alkaline  $pK_v$  values were approximately 3.20 and 6.20 in the first approach, in the second they shifted a little to 3.00 and 6.60 respectively (see *Table 4.6* and *Table 4.7*). As mentioned before, Asp and Glu have been acknowledged as the amino acids responsible for sucrose hydrolysis in *T. maritima* BfrA. Furthermore, since Glu works as a general acid/base, an abnormally high  $pK_a$  is expected. Therefore, estimated  $pK_v$  values agree with those of Asp and Glu.

**Table 4.6** Estimated  $pK_a$  values (2<sup>nd</sup> model, 1<sup>st</sup> approach)

	pH							
	4.56	5.10	5.56	6.08	6.63	7.20	7.68	8.03
$pK_{e1}$	3.50	2.30	2.30	2.30	2.30	2.30	2.30	2.30
$pK_{e2}$	5.50	5.82	5.72	5.61	6.01	5.92	5.94	5.89
$pK_{es1}$	2.20	2.30	2.30	2.30	2.30	2.30	2.30	2.30
$pK_{es2}$	6.21	6.21	6.22	6.24	6.26	6.28	6.30	6.30
$pK_{v1}$	3.25	3.26	3.26	3.26	3.26	3.26	3.26	3.26
$pK_{v2}$	6.21	6.21	6.22	6.24	6.26	6.28	6.30	6.30
$pK_{ess1}$	2.30	2.30	2.30	2.30	2.30	2.30	2.30	2.30
$pK_{ess2}$	5.77	5.78	5.66	6.44	5.74	5.94	6.11	5.67

**Table 4.7** Estimated  $pK_a$  values (2<sup>nd</sup> approach)

	2 <sup>nd</sup> model
$pK_{e1}$	4.69
$pK_{e2}$	6.00
$pK_{es1}$	4.23
$pK_{es2}$	6.00
$pK_{v1}$	3.00
$pK_{v2}$	6.60
$pK_{ess1}$	4.55
$pK_{ess2}$	6.00

The remaining alkaline  $pK_a$  values were very similar ranging from 5.50 to 6.00 in both approaches.

However, acidic  $pK_a$  values shifted from 2.30 in the first approach to approximately 4.50 in the second. In regard of these results one might be tempted to say that the amino acids involved in catalysis are likely to be the same as those implicated in substrate binding or inhibition. This statement, however, might not be completely true as previous determination of Glu did not come solely by linking its observed  $pK_a$  value to an ionizable group showed in *Table 4.2*. If this were the case, imidazole group from His should have been selected instead of Glu, which of course, would have been wrong.

From these observations it becomes clear that accurate identification of ionizable groups and their corresponding amino acids is rather difficult if ionization constants are the only information available. Since many ionizable groups at the active site have perturbed  $pK_a$  values, some even exhibiting shifts of 5 pH units (Harris & Turner, 2002), linear correlation with standard  $pK_a$  values reported is impractical. These perturbations come from electrostatic and close intermolecular interactions such as hydrogen bonding between nearby residues. Although  $pK_a$  alterations are present in every part of the enzyme, these are enhanced by the active site microenvironment. For instance, consider the electrostatic force between two interacting charges as explained by the Coulomb's Law:

$$F = \frac{q_1 q_2}{\epsilon r^2}$$

Therefore, the magnitude of electrostatic force ( $F$ ) between two ionizable groups at the active site will be proportional to the product of their charges ( $q$ ) and inversely proportional to the square of the distance ( $r^2$ ) between them and the dielectric constant ( $\epsilon$ ) of the medium. Although the latter is usually taken to be like that of water, at the active site this is greatly reduced given its hydrophobic environment which in turn enhances electrostatic interactions. Based on the crystal structure of *T. maritima* BfrA (Alberto et al., 2004), several amino acids in the active site vicinity could potentially be interacting with ionizable groups of those involved in catalysis (see *Table 4.8*).

**Table 4.8** Amino acids in close contact with sucrose at the active site of BfrA (Alberto et al., 2004)

Sucrose atom	Amino acid	Sucrose atom	Amino acid
Fructose O1	Asp-17*	Fructose C6	Phe-74
	Glu-190*	Fructose O6	Asn-16
	Trp-260		Gln-33
Fructose O2	Asn-16		Trp-41
	Asp-17*	Fructose C2	Asp-17*
Fructose O3	Arg-137	Glucose O1	Glu-190*
	Asp-138	Glucose O2	Tyr-240
	Glu-190*		Glu-190*
Fructose O4	Ser-75	Glucose O4	Arg-137
	Asp-138		

(\*) Catalytic amino acids

Since the influence of residue interaction is relevant for ionization constants, several approaches have been developed to combine not only enzyme kinetics but also mechanistic knowledge of enzyme's structure through either experimental data (i.e. X-ray crystallography), theoretical models or dedicated computational software packages (Alikhajeh et al., 2007; Nielsen & McCammon, 2003; Olivera-Nappa et al., 2004; S ndergaard et al., 2008).

Even though velocity equation developed in this study provided a limited estimation of ionization constants with no accurate information regarding its corresponding amino acids, it still proved to be a good guidance over the expected enzymatic activity at different pH and substrate conditions. For instance, considering the estimated Asp and Glu  $pK_a$  from the 2<sup>nd</sup> model (i.e. 3.00 and 6.60 respectively), favorable ionization state should be present when medium pH is between these values (S ndergaard et al., 2008). The latter is correlated with maximum activity showed by experimental data. Moreover, as pH approaches to more acidic values, a decrease in activity is expected since carboxylic group of Asp would become protonated making nucleophilic attack difficult. Again, this was clearly observed as negligible BfrA activity was measured below pH 4.5. Consequently, a similar decrease in enzymatic activity is also expected as pH increases and surpasses Glu  $pK_a$ . Since the latter would become mostly deprotonated, its ability to protonate sucrose's glycosidic bond would be impaired. However, if we look back to experimental data, we ascertain that this statement is only partially met as BfrA activity was indeed reduced but still measurable up to pH 8.0. In this regard, Yuan et al. (2012) have proposed that Glu is constantly being protonated by a nearby Arg residue ( $pK_a \sim 16$ ).

## Chapter 5. Conclusions

Kinetic characterization of *T. maritima* BfrA through a mathematical model and estimation of its kinetic parameters via LSNLR has been performed for the first time considering the simultaneous effects substrate inhibition and pH.

Production of recombinant strain of *E. coli* BL21 carrying the gene for BfrA and partial purification of the latter was achieved. Although the main focus of this study was not in the optimization of enzyme's recovery and purification yields, partially purified extract showed acceptable catalytic activity at 75°C (356 UI/mg) to carry on with further enzymatic characterization.

Initial velocity at 75 °C was obtained by assaying 11 and 12 levels of pH and substrate concentrations respectively. Experimental data showed that *T. maritima* BfrA suffered of uncompetitive inhibition by substrate after 146 mM of sucrose while its maximum activity was found between pH values of 4.5 and 5.5. At either acidic or alkaline conditions outside of this interval, enzymatic activity decrease was registered, though the latter was more pronounced for pH values below 4.5.

A velocity equation accounting for both effects of pH and uncompetitive inhibition by the substrate was established and fitted to initial velocity data following two different approaches: varying substrate concentration at fixed pH and varying both pH and substrate. A 1<sup>st</sup> model was obtained exhibiting good adjustment for the first approach and readily describing the effects of substrate inhibition. However, for the second approach the model suffered from lack of fit as well as insensitivity at alkaline conditions and substrate concentrations of 500 mM or more. A corrected 2<sup>nd</sup> model, with modified limits for estimation of ionization constants, improved its activity prediction and sensitivity as evidenced by its reduced sum of squared residuals.

Estimated  $K_m$  and  $K_i$  for both models were similar to those reported in the literature and showed slight variation with respect to pH. In contrast,  $v_{max}$  was quite sensitive to pH changes. Furthermore, acid ionization constants were more accurately estimated than those in the alkaline spectrum. Despite their similar sums of squares in the first approach, estimated parameters' standard deviation in 2<sup>nd</sup> model was reduced in comparison to the 1<sup>st</sup> model.

Calculated  $pK_a$  values for ionizable groups involved in catalysis yielded approximate values of 3.00 and 6.60 respectively, these correlated with those of Asp and Glu. Linkage of the latter to a high  $pK_a$  value was supported in previous studies of the enzyme's crystal structure as well as information of other glycosyl hydrolases with similar catalytic mechanisms.

Despite the 2<sup>nd</sup> model improvement with respect to the original, lack of adjustment and big standard deviation in estimated ionization constants were still noticeable when fitting to the second approach. Since  $pK_a$  are disturbed by close intermolecular interactions and these are particularly enhanced by the active site microenvironment, large standard deviation of estimated parameters is likely linked to insufficient structure-related data integrated into the velocity equation.

However, it should be noted that rather than constants values which remain unaltered, ionization 'constants' are more like dynamic built-in regulators of proteins and, of course, enzymes. Moreover, considering that an enzyme is constituted of several amino acids and each one of these has an intrinsic  $pK_a$  which is simultaneously affected by the medium pH and intermolecular interactions with neighboring residues, regulatory possibilities are immense.

Despite the limitations of the model developed in this study, it provided good indications with respect of expected enzymatic activity at different conditions of pH and sucrose concentrations.

Hence, proving its usefulness for further kinetic characterization studies with potential application in biocatalysis process design.

### ***Future work***

Firstly, optimization of production and purification process should be addressed to obtain higher yields of recombinant BfrA by testing different types of media formulations and culture conditions. Determination of the operational parameters' influence at each unit operation would be important to maximize both recovery and purity of the enzyme. Moreover, alternative purification trains should be explored as well as different formulation methodologies. Likewise, comparison between purified extracts would be desirable to evaluate the effect of contaminant proteins concentration in the catalytic activity.

The model proposed here should be refined with the findings of this work as well as additional information found in the literature. This new model should aim to both mitigate limitations over the lack of fit and provide more information regarding the intermolecular interaction between amino acids and their effect over ionizable groups involved in catalysis, substrate binding and inhibition. Alternatively, other methods of activity quantification and/or buffer systems should be implemented.

Finally, further stability assays such as determination of half live times at different temperatures and pH should be performed to obtain valuable information for enzymatic reactor design. Once a suitable velocity equation is obtained, the logical step to follow would be to test different immobilization procedures and the catalytic efficiency of *T. maritima* BfrA under heterogeneous kinetics to determine its potential use in industrial sucrose inversion.

## Appendix A

### Abbreviations and acronyms

**Table A.1** Abbreviations

	Description
<b>DNA</b>	Deoxyribonucleic acid
<b>BfrA</b>	$\beta$ -fructosidase
<b>SOB</b>	Super optimal broth
<b>SOC</b>	Super optimal broth with catabolite repression
<b>LB</b>	Luria Bertani
<b>OD<sub>600nm</sub></b>	Optical density at 600 nm
<b>DO</b>	Dissolved oxygen
<b>IPTG</b>	Isopropyl $\beta$ -D-1thiogalactopyranoside
<b>LEW</b>	Lysis-equilibration-wash
<b>CV</b>	Column volume
<b>dH<sub>2</sub>O</b>	Distilled water
<b>DNS</b>	3,5 dinitrosalicylic acid
<b>LSNLR</b>	Least-squares non-linear regression
<b>IMAC</b>	Immobilized metal affinity chromatography
<b>BSA</b>	Bovine serum albumin
<b>SDS-PAGE</b>	Sodium dodecyl sulfate – Polyacrylamide gel electrophoresis

**Table A.2** Acronyms

	Description
<b>IUBMB</b>	International Unit of Biochemistry and Molecular Biology
<b>INEGI</b>	Instituto Nacional de Estadística y Geografía

## Appendix B

### Variables and Symbols

**Table A.3** Variables and symbols

Variable	Description	Units
vvm	Aeration rate	$L_{\text{air}}/L_{\text{medium}} \cdot \text{min}$
IU	International unit of enzymatic activity	$\mu\text{mol}_{\text{Product}} / \text{min}$
$v_{\text{max}}$	Maximum velocity	$\text{IU} / \text{mg}_{\text{Protein}}$
$K_S$	Substrate affinity constant	$\text{mmol}_{\text{Substrate}} / \text{L}$
$K_m$	Michaelis-Menten constant	$\text{mmol}_{\text{Substrate}} / \text{L}$
$K_i$	Substrate inhibition constant	$\text{mmol}_{\text{Substrate}} / \text{L}$
$v_{\text{max}}^{\text{app}}$	Apparent maximum velocity	$\text{IU} / \text{mg}_{\text{Protein}}$
$K_m^{\text{app}}$	Michaelis-Menten constant	$\text{mmol}_{\text{Substrate}} / \text{L}$
$K_i^{\text{app}}$	Substrate inhibition constant	$\text{mmol}_{\text{Substrate}} / \text{L}$

## Appendix C

### Solutions and Buffers

**Table A.4** Polyacrylamide gel composition

	12.5% resolving gel	4% stacking gel
<b>dH<sub>2</sub>O</b>	1.6 mL	1.0 mL
<b>Acrylamide 30.8% (w/v)</b>	2.1 mL	220 µL
<b>1.5 M Tris HCl pH 8.8</b>	2.25 mL	-
<b>0.5 M Tris HCl pH 6.8</b>	-	415 µL
<b>SDS 10% (w/v)</b>	50 µL	16.5 µL
<b>APS 10% (w/v)</b>	30 µL	12.5 µL
<b>TEMED</b>	7.5 µL	3.75 µL

**Table A.5** 1X running buffer composition

	Concentration/Qty
<b>dH<sub>2</sub>O</b>	1 L
<b>Tris base</b>	0.606 % (w/v)
<b>Glycine</b>	2.883 % (w/v)
<b>SDS</b>	1 % (w/v)

**Table A.6** 2X sample buffer composition

	Concentration/Qty
<b>dH<sub>2</sub>O</b>	1.8 mL
<b>1.5 M Tris HCl pH 8.8</b>	3.0 mL
<b>SDS 10% (w/v)</b>	4.8 mL
<b>Glycerol</b>	2.4 mL
<b>Bromophenol blue</b>	0.012 % (w/v)

**Table A.7** Coomassie blue solution composition

	Concentration/Qty
<b>dH<sub>2</sub>O</b>	2 L
<b>Coomassie Blue R-250</b>	0.025 % (w/v)
<b>Methanol</b>	40 % (v/v)
<b>Acetic acid</b>	7 % (v/v)

**Table A.8** Destaining solutions composition

	Destaining solution I	Destaining solution II
<b>Ethanol</b>	50% (v/v)	-
<b>Acetic acid</b>	10% (v/v)	7% (v/v)
<b>Methanol</b>	-	5% (v/v)

**Table A.9** Enzymatic assay buffers compositions. All quantities expressed for 1 L volume.

<b>100 mM Citrate buffer pH 3.50</b>		<b>100 mM Phosphate buffer pH 6.20</b>	
Sodium citrate dihydrate	0.841 % (w/v)	Dibasic Sodium phosphate	0.129 % (w/v)
Citric acid	1.371 % (w/v)	Monobasic sodium phosphate monohydrate	1.254 % (w/v)
<b>100 mM Citrate buffer pH 4.00</b>		<b>100 mM Phosphate buffer pH 6.70</b>	
Sodium citrate dihydrate	1.198 % (w/v)	Dibasic Sodium phosphate	0.341 % (w/v)
Citric acid	1.138 % (w/v)	Monobasic sodium phosphate monohydrate	1.048 % (w/v)
<b>100 mM Citrate buffer pH 4.50</b>		<b>100 mM Phosphate buffer pH 7.20</b>	
Sodium citrate dihydrate	1.554 % (w/v)	Dibasic Sodium phosphate	0.710 % (w/v)
Citric acid	0.906 % (w/v)	Monobasic sodium phosphate monohydrate	0.690 % (w/v)
<b>100 mM Acetate buffer pH 4.70</b>		<b>100 mM Phosphate buffer pH 7.70</b>	
Sodium acetate	0.537 % (w/v)	Dibasic Sodium phosphate	1.078 % (w/v)
Acetic acid 99.7% (v/v)	0.217 % (v/v)	Monobasic sodium phosphate monohydrate	0.331 % (w/v)
<b>100 mM Acetate buffer pH 5.20</b>		<b>100 mM Tris-HCl buffer pH 8.90</b>	
Sodium acetate	0.696 % (w/v)	Tris base	1.211 % (w/v)
Acetic acid 99.7% (v/v)	0.091 % (v/v)	HCl 5M	0.333 % (v/v)
<b>100 mM Acetate buffer pH 5.60</b>		<b>100 mM Glycine-NaOH buffer pH 9.00</b>	
Sodium acetate	0.766 % (w/v)	Glycine	0.751 % (w/v)
Acetic acid 99.7% (v/v)	0.040 % (v/v)	NaOH 5M	0.274 % (v/v)
<b>100 mM Tris-Gly buffer pH 9.00</b>			
100 mM Tris-HCl buffer pH 8.90		50 % (v/v)	
100 mM Glycine-NaOH buffer pH 9.00		50 % (v/v)	

## Appendix D

### Production and Purification data

**Table A.10** Biomass determination

Time [h]	Biomass [g <sub>Dry weight</sub> /L]					
	Reactor 1			Reactor 2		
	1	2	Average	1	2	Average
0	0.320	0.700	0.510	0.480	0.140	0.310
1	0.320	0.280	0.300	0.400	0.420	0.410
2	1.780	ND	1.780	0.560	0.600	0.580
3	2.640	0.400	2.640	1.000	1.000	1.000
4	3.680	2.740	3.210	0.980	0.660	0.820
5	3.600	4.240	3.920	1.800	1.780	1.790
6	4.380	4.500	4.440	2.040	2.000	2.020
7	4.500	4.500	4.500	1.960	2.020	1.990
8	4.440	4.700	4.570	2.100	2.060	2.080

ND: Not determined

**Table A.11** Glucose consumption

Time [h]	Glucose [mg/mL]							
	Reactor 1				Reactor 2			
	1	2	3	Average	1	2	3	Average
0	8.162	8.729	8.426	8.439	9.244	8.869	9.498	9.204
1	9.099	8.873	10.144	9.372	9.828	9.379	9.068	9.425
2	8.124	8.535	8.306	8.322	8.764	8.739	8.618	8.707
3	6.651	6.802	7.612	7.022	6.538	6.485	6.582	6.535
4	3.471	3.445	3.512	3.476	5.405	5.310	5.252	5.322
5	1.474	1.441	1.490	1.468	2.682	2.682	2.660	2.675
6	ND	ND	ND	ND	ND	ND	ND	ND
7	0.245	0.229	0.232	0.235	0.273	0.260	0.268	0.267
8	0.209	0.207	0.210	0.209	0.163	0.163	0.164	0.163

ND: Not determined

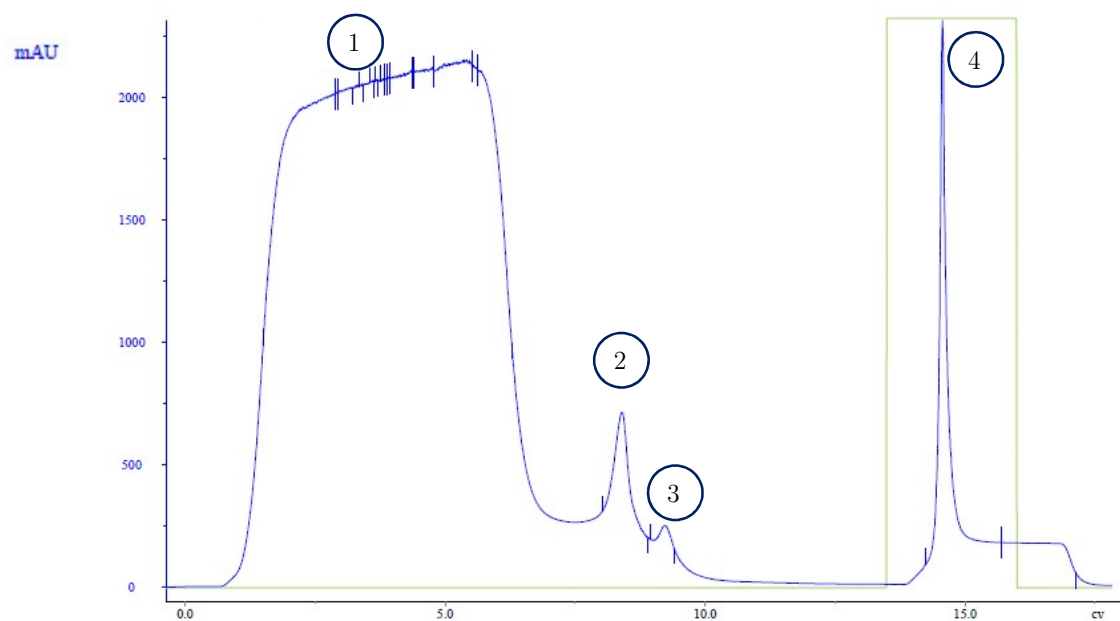


**Figure D.1** IMAC chromatogram. 1-3: Non-bound eluted peaks. 4: Eluted peak.

## Appendix E

Resulting plots of BfrA kinetic characterization

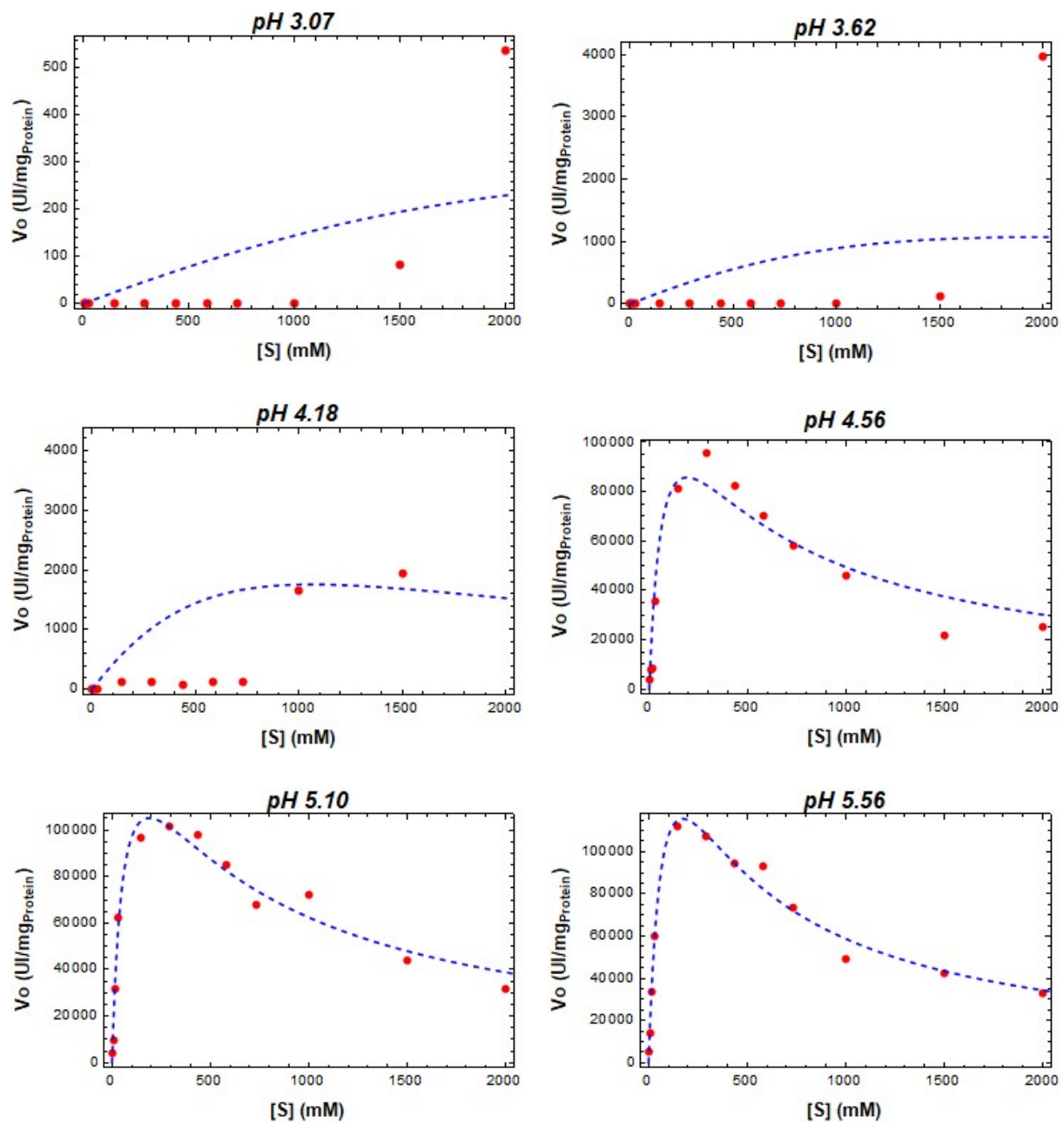


**Figure E.1** Initial velocity against substrate plots (fixed pH). Experimental data and the resulting model from LSNLR are represented by the red dots and dashed blue line respectively

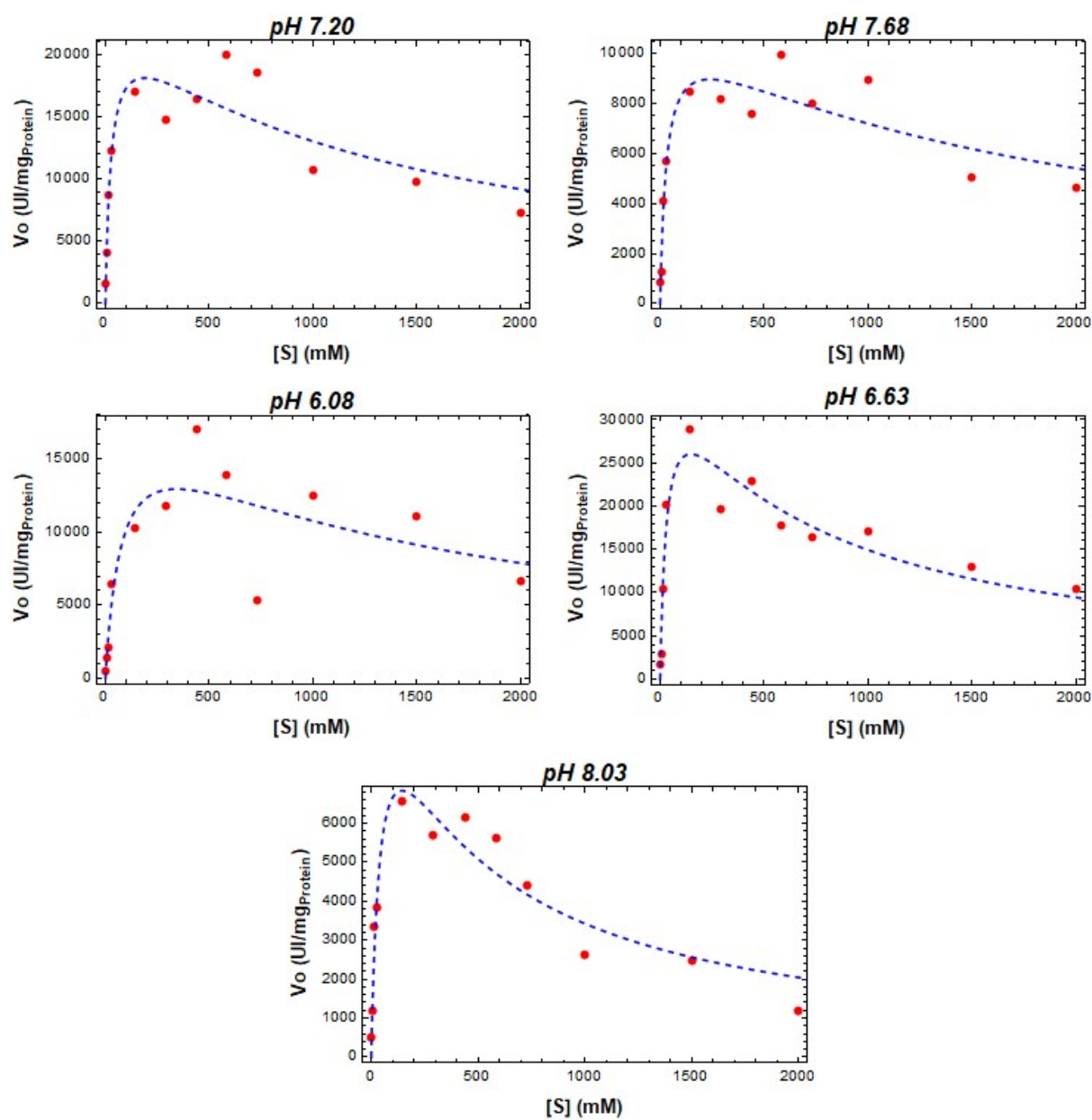


**Figure E.2 (Cont.)** Initial velocity against substrate plots (fixed pH). Experimental data and the resulting model from LSNLR are represented by the red dots and dashed blue line respectively

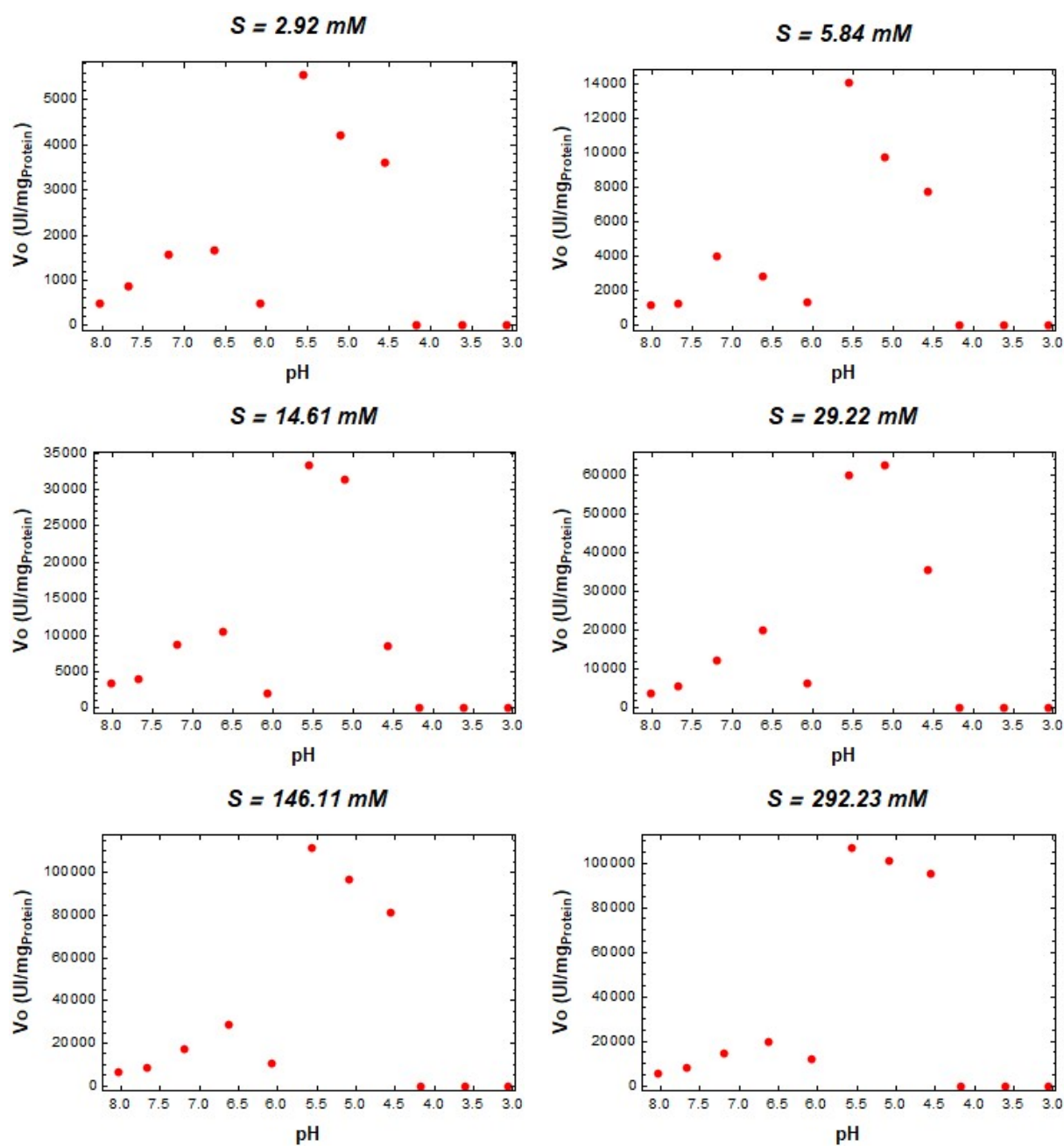


*Figure E.3* Initial velocity against pH plots (fixed substrate)

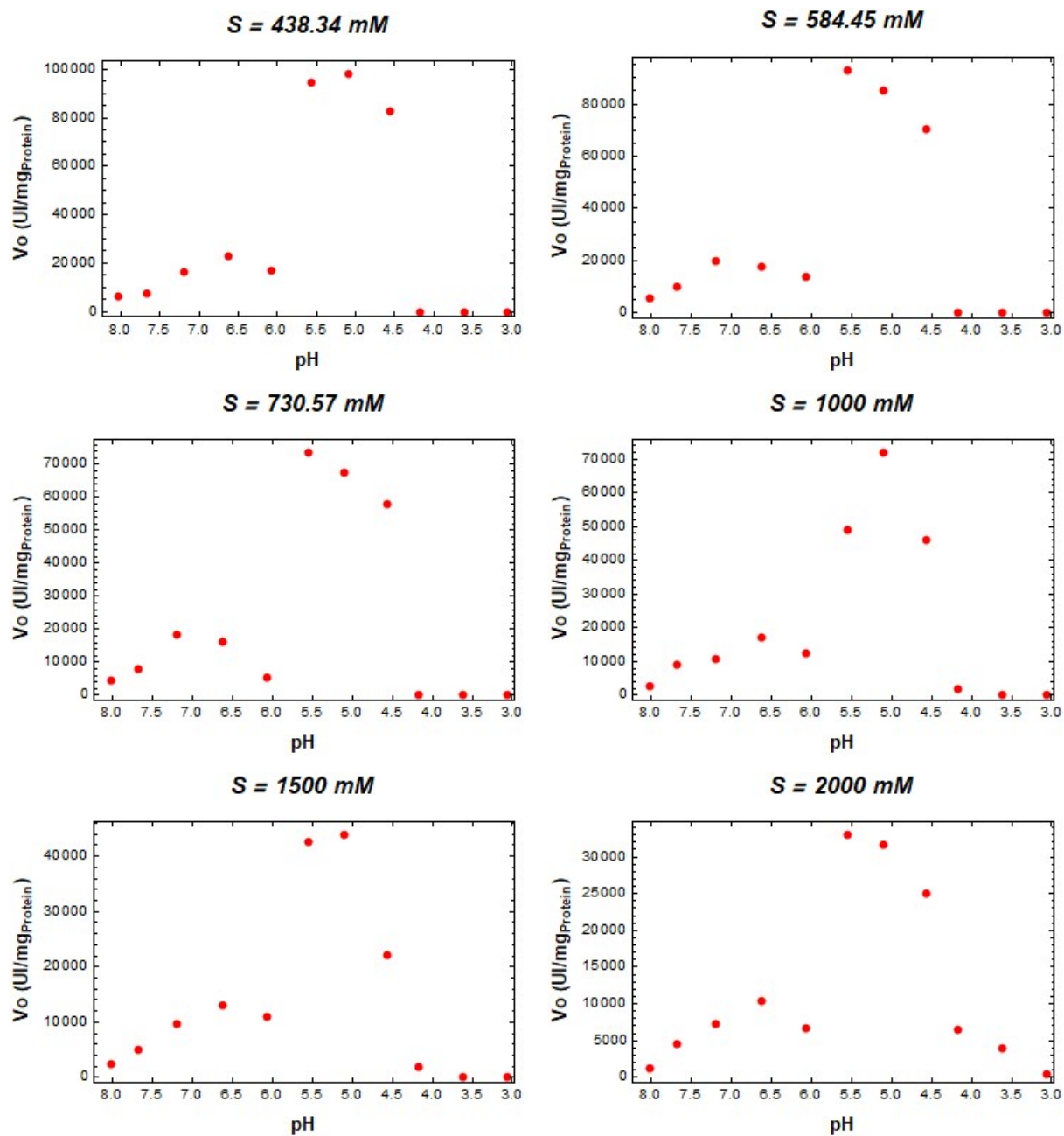


Figure E.4 (Cont.) Initial velocity against pH plots (fixed substrate)

## Bibliography

- Adams, M. W. W., Perler, F. B., & Kelly, R. M. (1995). Extremozymes: Expanding the Limits of Biocatalysis. *Nature Biotechnology*, 13(7), 662–668. <http://doi.org/10.1038/nbt0795-662>
- Ahmad, S., Anwar, A., & Saleemuddin, M. (2001). Immobilization and stabilization of invertase on Cajanus cajan lectin support. *Bioresource Technology*, 79(2), 121–127. [http://doi.org/10.1016/S0960-8524\(01\)00053-0](http://doi.org/10.1016/S0960-8524(01)00053-0)
- Akgöl, S., Kaçar, Y., Denizli, A., & Arca, M. Y. (2001). Hydrolysis of sucrose by invertase immobilized onto novel magnetic polyvinylalcohol microspheres. *Food Chemistry*, 74(3), 281–288. [http://doi.org/10.1016/S0308-8146\(01\)00150-9](http://doi.org/10.1016/S0308-8146(01)00150-9)
- Al-Haque, N., Santacoloma, P. A., Neto, W., Tufvesson, P., Gani, R., & Woodley, J. M. (2012). A robust methodology for kinetic model parameter estimation for biocatalytic reactions. *Biotechnology Progress*, 28(5), 1186–1196. <http://doi.org/10.1002/btpr.1588>
- Alberto, F., Bignon, C., Sulzenbacher, G., Henrissat, B., & Czjzek, M. (2004). The Three-dimensional Structure of Invertase ( $\beta$ -Fructosidase) from *Thermotoga maritima* Reveals a Bimodular Arrangement and an Evolutionary Relationship between Retaining and Inverting Glycosidases. *Journal of Biological Chemistry*, 279(18), 18903–18910. <http://doi.org/10.1074/jbc.M313911200>
- Alikhajeh, J., Khajeh, K., Naderi-Manesh, M., Ranjbar, B., Sajedi, R. H., & Naderi-Manesh, H. (2007). Kinetic analysis, structural studies and prediction of pKavalues of *Bacillus* KR-8104  $\alpha$ -amylase: The determinants of pH-activity profile. *Enzyme and Microbial Technology*, 41(3), 337–345. <http://doi.org/10.1016/j.enzmtec.2007.02.019>
- Amaya-Delgado, L., Hidalgo-Lara, M. E., & Montes-Horcasitas, M. C. (2006). Hydrolysis of sucrose by invertase immobilized on nylon-6 microbeads. *Food Chemistry*, 99(2), 299–304. <http://doi.org/10.1016/j.foodchem.2005.07.048>
- Arbige, M. V., & Pitcher, W. H. (1989). Industrial enzymology: a look towards the future. *Trends in Biotechnology*, 7(12), 330–335. [http://doi.org/10.1016/0167-7799\(89\)90032-2](http://doi.org/10.1016/0167-7799(89)90032-2)
- Ballou, G. A., & Luck, J. M. (1941). The effects of different buffers on the activity of activity  $\beta$ -amylase. *The Journal of Biological Chemistry*, 139, 233–240.

- Ballschmiter, M., Fütterer, O., & Liebl, W. (2006). Identification and characterization of a novel intracellular alkaline  $\alpha$ -amylase from the hyperthermophilic bacterium *Thermotoga maritima* MSB8. *Applied and Environmental Microbiology*, 72(3), 2206–11. <http://doi.org/10.1128/AEM.72.3.2206-2211.2006>
- Barroca, M., Santos, G., Johansson, B., Gillotin, F., Feller, G., & Collins, T. (2017). Deciphering the factors defining the pH-dependence of a commercial glycoside hydrolase family 8 enzyme. *Enzyme and Microbial Technology*, 96, 163–169. <http://doi.org/10.1016/j.enzmictec.2016.10.011>
- Bayramoglu, G., Doz, T., Ozalp, V. C., & Arica, M. Y. (2017). Improvement stability and performance of invertase via immobilization on to silanized and polymer brush grafted magnetic nanoparticles. *Food Chemistry*, 221, 1442–1450. <http://doi.org/10.1016/j.foodchem.2016.11.007>
- BBC-Business Communications Company Inc. (2009). *Report FOD020C-World markets for fermentation ingredients*. Wellesley, MA.
- Binod, P., Palkhiwala, P., Gaikawai, R., Madhavan Nampoothiri, K., Duggal, A., Dey, K., & Pandey, A. (2013). Industrial enzymes - Present status and future perspectives for india. *Journal of Scientific and Industrial Research*, 72(5), 271–286.
- Bommarius, A. S., & Paye, M. F. (2013). Stabilizing biocatalysts. *Chemical Society Reviews*, 42(15), 6534–6565. <http://doi.org/10.1039/c3cs60137d>
- Bowski, L., Saini, R., Ryu, D. Y., & Vieth, W. R. (1971). Kinetic modeling of the hydrolysis of sucrose by invertase. *Biotechnology and Bioengineering*, 13(5), 641–656. <http://doi.org/10.1002/bit.260130505>
- Briggs, G. E., & Haldane, J. B. (1925). A Note on the Kinetics of Enzyme Action. *The Biochemical Journal*, 19(2), 338–9. <http://doi.org/10.1042/BJ0190338>
- Cavaille, D., & Combes, D. (1995). Effect of temperature and pressure on yeast invertase stability: a kinetic and conformational study. *Journal of Biotechnology*, 43(3), 221–228. [http://doi.org/10.1016/0168-1656\(95\)00145-X](http://doi.org/10.1016/0168-1656(95)00145-X)
- Chen, Z., Chen, H., Ni, Z., Tian, R., Zhang, T., Jia, J., & Yang, S. (2015). Expression and characterization of a novel nitrilase from hyperthermophilic bacterium *thermotoga maritima* MSB8. *Journal of Microbiology and Biotechnology*, 25(10), 1660–1669. <http://doi.org/10.4014/jmb.1502.02032>
- Choi, J. M., Han, S. S., & Kim, H. S. (2015). Industrial applications of enzyme biocatalysis: Current status and future aspects. *Biotechnology Advances*, 33(7), 1443–1454.

- <http://doi.org/10.1016/j.biotechadv.2015.02.014>
- Clarke, M. A. (1995). Technological value of sucrose in food products. In *Sucrose: Properties and Applications* (pp. 223–247). Boston, MA: Springer US. [http://doi.org/10.1007/978-1-4615-2676-6\\_9](http://doi.org/10.1007/978-1-4615-2676-6_9)
- Cleland, W. W. (1967). The Statistical Analysis of Enzyme Kinetic Data. In *Advances in enzymology and related areas of molecular biology* (pp. 1–32). Wiley-Blackwell. <http://doi.org/10.1002/9780470122747.ch1>
- Cleland, W. W. (1977). Determining the Chemical Mechanisms of Enzyme-Catalyzed Reactions by Kinetic Studies. In *Advances in Enzymology and Related Areas of Molecular Biology* (pp. 273–387). Wiley-Blackwell. <http://doi.org/10.1002/9780470122907.ch4>
- Cleland, W. W. (1982). [22] The use of pH studies to determine chemical mechanisms of enzyme-catalyzed reactions. In *Methods in Enzymology* (Vol. 87, pp. 390–405). [http://doi.org/10.1016/S0076-6879\(82\)87024-9](http://doi.org/10.1016/S0076-6879(82)87024-9)
- Combes, D., & Monsan, P. (1983). Sucrose hydrolysis by invertase. Characterization of products and substrate inhibition. *Carbohydrate Research*, 117(C), 215–228. [http://doi.org/10.1016/0008-6215\(83\)88088-4](http://doi.org/10.1016/0008-6215(83)88088-4)
- Davies, G., & Henrissat, B. (1995). Structures and mechanisms of glycosyl hydrolases. *Structure*, 3(9), 853–859.
- Demirjian, D. C., Morís-Varas, F., & Cassidy, C. S. (2001). Enzymes from extremophiles. *Current Opinion in Chemical Biology*, 5(2), 144–151. [http://doi.org/10.1016/S1367-5931\(00\)00183-6](http://doi.org/10.1016/S1367-5931(00)00183-6)
- Di Cosimo, R., Mc Auliffe, J., Poulose, A. J., & Bohlmann, G. (2013). Industrial use of immobilized enzymes. *Chemical Society Reviews*, 42(15), 6437–6474. <http://doi.org/10.1039/c3cs35506c>
- Dickensheets, P. A., Chen, L. F., & Tsao, G. T. (1977). Characteristics of yeast invertase immobilized on porous cellulose beads. *Biotechnology and Bioengineering*, 19(3), 365–375. <http://doi.org/10.1002/bit.260190307>
- Edwards, W. P. (Bill). (2009). Caramels, fondants and jellies as centres and fillings. *Science and Technology of Enrobed and Filled Chocolate, Confectionery and Bakery Products*, 123–151. <http://doi.org/10.1533/9781845696436.1.123>
- Elleuche, S., Schäfers, C., Blank, S., Schröder, C., & Antranikian, G. (2015). Exploration of extremophiles for high temperature biotechnological processes. *Current Opinion in Microbiology*, 25, 113–119.

- <http://doi.org/10.1016/j.mib.2015.05.011>
- Elleuche, S., Schröder, C., Sahm, K., & Antranikian, G. (2014). Extremozymes-biocatalysts with unique properties from extremophilic microorganisms. *Current Opinion in Biotechnology*, 29(1), 116–123. <http://doi.org/10.1016/j.copbio.2014.04.003>
- Garcia-Galan, C., Berenguer-Murcia, Á., Fernandez-Lafuente, R., & Rodrigues, R. C. (2011). Potential of different enzyme immobilization strategies to improve enzyme performance. *Advanced Synthesis and Catalysis*, 353(16), 2885–2904. <http://doi.org/10.1002/adsc.201100534>
- Garriga, M., Almaraz, M., Marchiaro, A., Nacional De La, U., San, P., Bosco, J., & Rivadavia -Argentina, C. (2017). Determination of reducing sugars in extracts of *Undaria pinnatifida* (harvey) algae by UV-visible spectrophotometry (DNS method). *Actas de Ingeniería*, 3, 173–179. Retrieved from <http://fundacioniai.org/actas>
- Gomes, J., & Steiner, W. (2004). The biocatalytic potential of extremophiles and extremozymes. *Food Technology and Biotechnology*, 42(4), 223–235.
- Gurung, N., Ray, S., Bose, S., & Rai, V. (2013). A broader view: Microbial enzymes and their relevance in industries, medicine, and beyond. *BioMed Research International*, 2013. <http://doi.org/10.1155/2013/329121>
- Harris, T. K., & Turner, G. J. (2002). Structural Basis of Perturbed pKa Values of Catalytic Groups in Enzyme Active Sites. *IUBMB Life*, 53(2), 85–98. <http://doi.org/10.1080/10399710290038972>
- Henri, V. (1902). Théorie générale de l'action de quelques diastases. *C. R. Hebd. Acad. Sci.*, 135, 916–919.
- Herrera, V., Ticona, J. C., Udaeta, E., & Chuqui, R. (2008). Validación del método analítico para la cuantificación de alcaloides quinolínicos del extracto de *Galipea longiflora* Krause Kallunki Analytic method validation for the quantification of quinolinical alkaloid in extracts from *Galipea longiflora* Krause Kall. *Biofarbo*, 16, 47–53. <http://doi.org/10.1080/13841280601124955>
- Illanes, A. (2008). *Enzyme Biocatalysis: Principles and applications*. (A. Illanes, Ed.). Springer Science & Business Media.
- INEGI. (2014a). *Balanza comercial de mercancías de México. Anuario estadístico 2014. Importaciones pesos*. Retrieved from [www.inegi.org.mx](http://www.inegi.org.mx)
- INEGI. (2014b). *Balanza comercial de mercancías de México. Anuario estadístico 2014. Exportaciones pesos*.

Retrieved from [www.inegi.org.mx](http://www.inegi.org.mx)

- Jemli, S., Ayadi-Zouari, D., Hlima, H. Ben, & Bejar, S. (2016). Biocatalysts: Application and engineering for industrial purposes. *Critical Reviews in Biotechnology*, 36(2), 246–258. <http://doi.org/10.3109/07388551.2014.950550>
- Johnson, K. A. (2013). A century of enzyme kinetic analysis, 1913 to 2013. *FEBS Letters*, 587(17), 2753–2766. <http://doi.org/10.1016/j.febslet.2013.07.012>
- Keramat, A., Kargari, A., Sohrabi†, M., Mirshekar, H., & Sanaeepur, H. (2017). A kinetic model for invertase-induced sucrose hydrolysis: considering the initial time lag. *Chemical Engineering & Technology*, 40(3), 529–536. <http://doi.org/https://doi.org/10.1002/ceat.201400389>
- Kern, G., Schulke, N., Schmid, F. X., & Jaenicke, R. (1992). Internal , External , and Core-Glycosylated Invertase From Yeast. *Protein Science*, 1(1), 120–131.
- Khan, M. A. S., Akbar, M., Kitaoka, M., & Hayashi, K. (2007). A unique thermostable lichenase from *Thermotoga maritima* MSB8 with divergent substrate specificity. *Indian Journal of Biotechnology*, 6(3), 315–320.
- Kirk, O., Borchert, T. V., & Fuglsang, C. C. (2002). Industrial enzyme applications. *Current Opinion in Biotechnology*, 13(4), 345–351. [http://doi.org/10.1016/S0958-1669\(02\)00328-2](http://doi.org/10.1016/S0958-1669(02)00328-2)
- Knowles, A. J. R. (1976). The intrinsic pKa values of functional groups in enzymes: Improper deductions from the pH-dependence of steady-state parameters. *CRC Critical Reviews in Biochemistry*, 4(2), 165–173.
- Koshland, D. E., & Stein, S. (1954). Correlation of bond breaking with enzyme specificity. Cleavage point of invertase. *Journal of Biological Chemistry*, 208(1), 139–148.
- Kudo, K., Watanabe, A., Ujiie, S., Shintani, T., & Gomi, K. (2015). Purification and enzymatic characterization of secretory glycoside hydrolase family 3 (GH3) aryl  $\beta$ -glucosidases screened from *Aspergillus oryzae* genome. *Journal of Bioscience and Bioengineering*, 120(6), 614–623. <http://doi.org/10.1016/j.jbiosc.2015.03.019>
- Leskovac, V. (2003). The pH Dependence of Enzyme Catalysis. In *Comprehensive Enzyme Kinetics* (pp. 283–315). Boston: Kluwer Academic Publishers. [http://doi.org/10.1007/0-306-48390-4\\_14](http://doi.org/10.1007/0-306-48390-4_14)
- Liebl, W., Brem, D., & Gotschlich, A. (1998). Analysis of the gene for  $\beta$ -fructosidase (invertase, inulinase) of the hyperthermophilic bacterium *Thermotoga maritima*, and characterisation of the enzyme expressed

- in *Escherichia coli*. *Applied Microbiology and Biotechnology*, 50(1), 55–64.  
<http://doi.org/10.1007/s002530051256>
- Liu, Q., Xun, G., & Feng, Y. (2018). The state-of-the-art strategies of protein engineering for enzyme stabilization. *Biotechnology Advances*, #pagerange#. <http://doi.org/10.1016/J.BIOTECHADV.2018.10.011>
- Lodish, H., Berk, A., Kaiser, C. A., Krieger, M., Scott, M. P., Bretscher, A., & Ploegh, H. (2008). *Molecular Cell Biology*. New York: W H Freeman.
- Mafrá, A. C. O., Beltrame, M. B., Ulrich, L. G., Giordano, R. de L. C., Ribeiro, M. P. de A., & Tardioli, P. W. (2018). Combined CLEAs of invertase and soy protein for economically feasible conversion of sucrose in a fed-batch reactor. *Food and Bioprocess Processing*, 110, 145–157.  
<http://doi.org/10.1016/j.fbp.2018.05.006>
- Markets and Markets. (2017). Industrial Enzymes Market - Global Forecast by 2022. Retrieved October 17, 2018, from <https://www.marketsandmarkets.com/PressReleases/industrial-enzymes.asp>
- Martínez, D., Cutiño-Avila, B., Pérez, E. R., Menéndez, C., Hernández, L., & Del Monte-Martínez, A. (2014). A thermostable exo- $\beta$ -fructosidase immobilised through rational design. *Food Chemistry*, 145, 826–831.  
<http://doi.org/10.1016/j.foodchem.2013.08.073>
- Mateo, C., Palomo, J. M., Fernandez-Lorente, G., Guisan, J. M., & Fernandez-Lafuente, R. (2007). Improvement of enzyme activity, stability and selectivity via immobilization techniques. *Enzyme and Microbial Technology*, 40(6), 1451–1463. <http://doi.org/10.1016/j.enzmictec.2007.01.018>
- Menéndez, C., Martínez, D., Trujillo, L. E., Mazola, Y., González, E., Pérez, E. R., & Hernández, L. (2013). Constitutive high-level expression of a codon-optimized  $\beta$ -fructosidase gene from the hyperthermophile *Thermotoga maritima* in *Pichia pastoris*. *Applied Microbiology and Biotechnology*, 97(3), 1201–1212.  
<http://doi.org/10.1007/s00253-012-4270-2>
- Michaelis, L., & Menten, M. L. (1913). Die Kinetik der Invertinwirkung. *Biochem Z*, 49(February), 333–369.  
<http://doi.org/10.1021/bi201284u>
- Miller, G. L. (1959). Use of Dinitrosalicylic Acid Reagent for Determination of Reducing Sugar. *Analytical Chemistry*, 31(3), 426–428. <http://doi.org/10.1021/ac60147a030>
- Mohandesi, N., Haghbeen, K., Ranaei, O., Arab, S. S., & Hassani, S. (2017). Catalytic efficiency and

- thermostability improvement of Suc2 invertase through rational site-directed mutagenesis. *Enzyme and Microbial Technology*, 96, 14–22. <http://doi.org/10.1016/j.enzmictec.2016.09.004>
- Monsan, P., & Combes, D. (1984). Application of immobilized invertase to continuous hydrolysis of concentrated sucrose solutions. *Biotechnology and Bioengineering*, 26(4), 347–351. <http://doi.org/10.1002/bit.260260409>
- Moss, G. P. (2018). IUBMB Nomenclature Home Page. Retrieved October 13, 2018, from <http://www.sbcs.qmul.ac.uk/iubmb/>
- Nadeem, H., Rashid, M. H., Siddique, M. H., Azeem, F., Muzammil, S., Javed, M. R., ... Riaz, M. (2015). Microbial invertases: A review on kinetics, thermodynamics, physiochemical properties. *Process Biochemistry*, 50(8), 1202–1210.
- Nelson, K. E., Clayton, R. a, Gill, S. R., Gwinn, M. L., Dodson, R. J., Haft, D. H., ... Fraser, C. M. (1999). Evidence for lateral gene transfer between Archaea and bacteria from genome sequence of *Thermotoga maritima*. *Nature*, 399(6734), 323–329. <http://doi.org/10.1038/20601>
- Nielsen, J. E., & McCammon, J. A. (2003). Calculating pKa values in enzyme active sites. *Protein Science*, 12(9), 1894–1901. <http://doi.org/10.1110/ps.03114903>
- Olivera-Nappa, A., Andrews, B. A., & Asenjo, J. A. (2004). A mixed mechanistic-electrostatic model to explain pH dependence of glycosyl hydrolase enzyme activity. *Biotechnology and Bioengineering*, 86(5), 573–586. <http://doi.org/10.1002/bit.20063>
- Paine, H. S., Walton Jr., C. F., & Badollet, M. S. (1925). Industrial Applications of Invertase. *Industrial & Engineering Chemistry*, 17(5), 445–450.
- Pek, H. Bin, Klement, M., Ang, K. S., Chung, B. K. S., Ow, D. S. W., & Lee, D. Y. (2015). Exploring codon context bias for synthetic gene design of a thermostable invertase in *Escherichia coli*. *Enzyme and Microbial Technology*, 75–76, 57–63. <http://doi.org/10.1016/j.enzmictec.2015.04.008>
- Rajashekhara, E., Kitaoka, M., Kim, Y.-K., & Hayashi, K. (2002). Characterization of a Cellobiose Phosphorylase from a Hyperthermophilic Eubacterium, *Thermotoga maritima* MSB8. *Bioscience, Biotechnology, and Biochemistry*, 66(12), 2578–2586. <http://doi.org/10.1271/bbb.66.2578>
- Rampp, M., Buttersack, C., & Lüdemann, H. D. (2000). c,T-dependence of the viscosity and the self-diffusion coefficients in some aqueous carbohydrate solutions. *Carbohydrate Research*, 328(4), 561–572.

- [http://doi.org/10.1016/S0008-6215\(00\)00141-5](http://doi.org/10.1016/S0008-6215(00)00141-5)
- Reddy, V. A., & Maley, F. (1990). Residue in Yeast Invertase by Affinity Labeling and Site- directed Mutagenesis. *Biochemistry*, 265(19), 10817–10820.
- Reddy, V. A., & Maley, F. (1996). Studies on identifying the catalytic role of Glu-204 in the active site of yeast invertase. *Journal of Biological Chemistry*, 271(24), 13953–13958. <http://doi.org/10.1074/jbc.271.24.13953>
- Rodrigues, R. C., Ortiz, C., Berenguer-Murcia, Á., Torres, R., & Fernández-Lafuente, R. (2013). Modifying enzyme activity and selectivity by immobilization. *Chemical Society Reviews*, 42(15), 6290–6307. <http://doi.org/10.1039/c2cs35231a>
- Rosano, G. L., & Ceccarelli, E. A. (2014). Recombinant protein expression in Escherichia coli: Advances and challenges. *Frontiers in Microbiology*, 5(APR), 1–17. <http://doi.org/10.3389/fmicb.2014.00172>
- Sanchez, S., & Demain, A. L. (2016). *Useful Microbial Enzymes-An Introduction. Biotechnology of Microbial Enzymes: Production, Biocatalysis and Industrial Applications* (Vol. 2017). Elsevier Inc. <http://doi.org/10.1016/B978-0-12-803725-6.00001-7>
- Sarrouh, B. (2012). Up-To-Date Insight on Industrial Enzymes Applications and Global Market. *Journal of Bioprocessing & Biotechniques*, s1(01). <http://doi.org/10.4172/2155-9821.S4-002>
- Segel, I. H. (1975). *Enzyme Kinetics: Behavior and Analysis of Rapid Equilibrium and Steady-State Enzyme Systems*. John Wiley & Sons.
- Siddiqui, K. S. (2015). Some like it hot, some like it cold: Temperature dependent biotechnological applications and improvements in extremophilic enzymes. *Biotechnology Advances*, 33(8), 1912–1922. <http://doi.org/10.1016/j.biotechadv.2015.11.001>
- Silva, C., Martins, M., Jing, S., Fu, J., & Cavaco-Paulo, A. (2018). Practical insights on enzyme stabilization. *Critical Reviews in Biotechnology*, 38(3), 335–350. <http://doi.org/10.1080/07388551.2017.1355294>
- Singh, R., Kumar, M., Mittal, A., & Mehta, P. K. (2016). Microbial enzymes: industrial progress in 21st century. *3 Biotech*, 6(2), 1–15. <http://doi.org/10.1007/s13205-016-0485-8>
- Søndergaard, C. R., McIntosh, L. P., Pollastri, G., & Nielsen, J. E. (2008). Determination of Electrostatic Interaction Energies and Protonation State Populations in Enzyme Active Sites. *Journal of Molecular Biology*, 376(1), 269–287. <http://doi.org/10.1016/j.jmb.2007.09.070>

- Sun, F., Zhang, X. Z., Myung, S., & Zhang, Y. H. P. (2012). Thermophilic *Thermotoga maritima* ribose-5-phosphate isomerase RpiB: Optimized heat treatment purification and basic characterization. *Protein Expression and Purification*, 82(2), 302–307. <http://doi.org/10.1016/j.pep.2012.01.017>
- Sweeney, M. D., & Xu, F. (2012). Biomass Converting Enzymes as Industrial Biocatalysts for Fuels and Chemicals: Recent Developments. *Catalysts*, 2(4), 244–263. <http://doi.org/10.3390/catal2020244>
- Tananchai, P., & Chisti, Y. (2010). Stabilization of invertase by molecular engineering. *Biotechnology Progress*, 26(1), 111–117. <http://doi.org/10.1002/btpr.314>
- Valerio, S. G., Alves, J. S., Klein, M. P., Rodrigues, R. C., & Hertz, P. F. (2013). High operational stability of invertase from *Saccharomyces cerevisiae* immobilized on chitosan nanoparticles. *Carbohydrate Polymers*, 92(1), 462–468. <http://doi.org/10.1016/j.carbpol.2012.09.001>
- Van den Burg, B. (2003). Extremophiles as a source for novel enzymes. *Current Opinion in Microbiology*, 6(3), 213–218. [http://doi.org/10.1016/S1369-5274\(03\)00060-2](http://doi.org/10.1016/S1369-5274(03)00060-2)
- Vaughan, D., & Malcolm, R. E. (1984). Influence of assay conditions on invertase activity in different Scottish soils. *Plant and Soil*, 80(2), 285–292. <http://doi.org/10.1007/BF02161184>
- Whitehurst, R. J., & van Oort, M. (2009). *Enzymes in Food Technology*. (R. J. Whitehurst & M. van Oort, Eds.). Oxford, UK: Wiley-Blackwell. <http://doi.org/10.1002/9781444309935>
- Wohlgemuth, R. (2010). Biocatalysis-key to sustainable industrial chemistry. *Current Opinion in Biotechnology*, 21(6), 713–724. <http://doi.org/10.1016/j.copbio.2010.09.016>
- Woodley, J. M. (2013). Protein engineering of enzymes for process applications. *Current Opinion in Chemical Biology*, 17(2), 310–316. <http://doi.org/10.1016/j.cbpa.2013.03.017>
- Yuan, S., Le Roy, K., Venken, T., Lammens, W., van den Ende, W., & de Maeyer, M. (2012). PKa modulation of the Acid/Base catalyst within GH32 and GH68: A role in substrate/inhibitor specificity? *PLoS ONE*, 7(5), 1–12. <http://doi.org/10.1371/journal.pone.0037453>
- Zechel, D. L., & Withers, S. G. (2000). Glycosidase Mechanisms: Anatomy of a Finely Tuned Catalyst. *Accounts of Chemical Research*, 33(1), 11–18. Retrieved from <http://search.ebscohost.com/login.aspx?direct=true&AuthType=ip,shib&db=jlh&AN=128387585&sit e=ehost-live>

## Submitted works

IX Congreso de Biotecnología y Bioingeniería del Sureste at UADY<sup>1</sup>, October 2018, Merida, YUC,MX

Memoria in extenso. Biotecnología Enzimática-Biocatálisis

IX Congreso de Biotecnología y Bioingeniería del Sureste. Mérida, Yucatán del 24 al 26 de octubre de 2018. 05-08 pp.

### PRODUCCIÓN, PURIFICACIÓN Y CARACTERIZACIÓN CINÉTICA DE UNA INVERTASA EXTREMÓFILA RECOMBINANTE

Juan Jesús Cruz-Maldonado<sup>1</sup>, Lucero Alondra Jiménez Martínez<sup>1</sup>, Alicia Ramírez Medrano<sup>2</sup> y Carlos Eduardo Gómez-Sánchez<sup>1</sup>,

<sup>1</sup>Instituto Tecnológico de Estudios Superiores de Monterrey Campus Toluca. Eduardo Monroy Cárdenas 2000, San Antonio Buenavista, C.P. 50110. Toluca de Lerdo, Estado de México, México.

<sup>2</sup>Instituto Tecnológico de Estudios Superiores de Monterrey Campus Ciudad de México. Calle del Puente #222 Col. Ejidos de Huipulco, Tlalpan C.P. 14380, México D.F., México.

\*Autor de correspondencia: carlos.eduardo.gomez@itesm.mx

Recibido: 31/agosto/2018

Aceptado: 30/septiembre/2018

Publicado: 31/octubre/2018

### INTRODUCCIÓN

En procesos industriales de síntesis química se utilizan catalizadores inorgánicos que requieren de condiciones extremas de pH, temperatura y presión. Estos tienen las desventajas de tener baja eficiencia catalítica y especificidad. En contraste, las enzimas pueden trabajar a condiciones mucho más moderadas y presentan beneficios importantes en cuanto a especificidad y rendimiento. Así mismo, con la tendencia actual por el desarrollo de procesos sustentables, las enzimas han recibido una mayor atención para ser incorporados en diversos procesos industriales (Adrio y Demain, 2014). Sin embargo, no todas las enzimas se pueden adecuar tan fácilmente a las condiciones de temperatura, presión, pH y concentración de sustrato o productos exigidas por un proceso para ser considerados como redituables (Jemli et al., 2016). Desde la perspectiva de los procesos industriales, el uso de enzimas que puedan operar y mantenerse estables a condiciones drásticas de proceso, como aquellas de los organismos extremófilos, impacta de forma positiva en la reducción de los costos de producción, operación de equipos y subsecuente purificación de la molécula o metabolito objetivo.

La producción industrial de sacarosa invertida, que de forma rutinaria es catalizada por la enzima  $\beta$ -fructosidasa (BfrA) de la levadura mesofílica *Saccharomyces cerevisiae*, se lleva a cabo en reactores enzimáticos a temperaturas entre 55°C y 70°C y a altas concentraciones de sustrato (60% (p/v)) (Menéndez et al., 2013). Sin embargo, a estas condiciones la enzima no solo opera bajo inhibición por sustrato, sino que también se encuentra fuera de su intervalo de estabilidad térmica y se desnaturaliza de forma irreversible (Cavaille y Combes, 1995) lo cual resulta tanto en reducción del rendimiento de reacción como en encarecimiento de los costos de producción y operación.

Llevar a cabo reacciones enzimáticas a altas temperaturas (>60°C) trae consigo beneficios como el aumento de ambos, la solubilidad y el coeficiente de difusión del sustrato, así como la reducción de la viscosidad, lo que resulta en un incremento de las velocidades de transferencia másica y de reacción, sin mencionar una menor probabilidad de contaminación (Gomes y Steiner, 2004). No obstante, la baja estabilidad a altas temperaturas es una de las desventajas más comunes a la hora de incorporar biocatalizadores en procesos industriales. En este sentido, los organismos extremófilos y específicamente aquellos capaces de desarrollarse a temperaturas elevadas (60-80°C) o termófilos, se han presentado recientemente como una fuente natural y atractiva para la obtención de biocatalizadores térmicamente estables (Elleuche et al., 2015). En el caso particular de la BfrA se tiene el precedente de la enzima obtenida a partir de *Thermotoga maritima* MSB8 (Liebl et al., 1998) cuya temperatura óptima de reacción ronda los 90-95°C haciéndola adecuada para las condiciones de temperatura anteriormente mencionadas.

Por otro lado, un aspecto importante para el diseño de reactores enzimáticos consiste en conocer el efecto de los diferentes parámetros de operación como pH, temperatura y especialmente la concentración de sustrato sobre la velocidad de reacción. Este efecto puede entenderse mediante la siguiente ecuación de velocidad (Ec. 1)

$$v = \frac{v_{max}[S]}{K_m + [S] \left( 1 + \frac{[S]}{K_i} \right)} \quad (Ec. 1)$$

Donde [S] es la concentración de sustrato,  $v_{max}$  es la velocidad máxima de reacción,  $K_m$  la constante de afinidad por el sustrato y  $K_i$  la constante de inhibición del sustrato. La determinación de los parámetros cinéticos de la ecuación de velocidad no solo proporcionará una mayor comprensión del mecanismo catalítico de la enzima, sino que también servirá como punto de partida para el diseño de reactores enzimáticos (Bowski et al., 1971). Por tal motivo, el objetivo del presente trabajo es caracterizar cinéticamente a la BfrA recombinante de *T. maritima* MSB8 expresada en *E. coli* BL21.

<sup>1</sup><http://www.ingquimica.uady.mx/sitios/smbb2018/>

## Curriculum Vitae

Juan Jesús Cruz Maldonado was born in Atlacomulco, Mexico, Mexico, on December 1<sup>st</sup>, 1990. He earned the Biotechnology Engineering degree from the *Instituto Tecnológico y de Estudios Superiores de Monterrey*, Campus Toluca in December 2012. For the next three years he labored at Laboratorios Silanes' sister biopharmaceutical company Instituto Bioclon. There he worked at as bioprocess engineer and, later on, as production supervisor performing activities such as operating personnel training, Standard Operation Procedures elaboration, acquisition of materials and equipment as well as design, implementation and supervision of antivenom purification processes.

Continuing with his professional education Juan was accepted in the Master of Science graduate program of the *Instituto Tecnológico y de Estudios Superiores de Monterrey*, Campus Monterrey in January 2016. There, under the tutelage of Dr. Alicia Ramírez and M. Sc. Carlos Gómez, he was given the opportunity to complement its professional training by designing and implementing a mathematical model to describe enzymatic catalytic behavior under the effect of pH. Which led him to combine technical laboratory techniques (i.e. spectrophotometric, enzymatic and analytical assays) with engineer-oriented computational software.

This document was typed in using Microsoft Word  
by Juan Jesús Cruz Maldonado